NATIONAL ADVISORY COMMITTEE FOR AERONAUTICS

MEMORANDUM REPORT

for the

Air Technical Service Command, Army Air Forces

INVESTIGATION OF TYPICAL HIGH-SPEED BOMBER WING IN THE LANGLEY 8-FOOT HIGH-SPEED TUNNEL

Part I

Wing Characteristics

By Richard T. Whitcomb

Langley Memorial Aeronautical Laboratory
Langley Field, Va.

May 29, 1945

NATIONAL ADVISORY COMMITTEE FOR AERONAUTICS

MEMORANDUM REPORT

for the

Air Technical Service Command, Army Air Forces

INVESTIGATION OF TYPICAL HIGH-SPEED BOMBER WING IN THE LANGLEY 8-FOOT HIGH-SPEED TUNNEL

Part I

Wing Characteristics

By Richard T. Whitcomb

Langley Memorial Aeronautical Laboratory
Langley Field, Va.

May 29, 1945

SUMMARY

A series of high-speed tests have been made on a typical high-speed bomber wing in the Langley 8-foot high-speed wind tunnel at Mach numbers up to 0.90. The model tested has an aspect ratio of 9.0, a taper ratio of 2.5 to 1.0, no twist, dihedral, or sweepback. It has 20-percent chord, 40-percent-semispan plain ailerons. The present report presents the results of the test of the wing alone with 0° aileron deflections. The results indicate that there are substantial changes in the normal forces, pitching moments, drags, root-bending moments and wake widths at the tail position when the Mach number is increased beyond the point of force break which varies from a Mach number of 0.73 at the high angles of attack to a Mach number of 0.80 at an angle of 0° degrees. These changes will produce serious effects on the trim and stability of an airplane and will alter the requirements for the airplane structure.

INTRODUCTION

At the request of the Air Technical Service Command, Army Air Forces, the NACA has undertaken a general research program in conjunction with the design of a high-speed bomber. It was decided at a conference between representatives of the Air Technical Service Command, the NACA, and the manufacturers concerned, that the Langley 8-foot high-speed wind tunnel would test a model of a typical bomber wing in order to establish the effects of compressibility at the extremely high speed proposed for this airplane. The tests of this wing were to be made to determine the characteristics of the wing alone, the wing with dive-control devices, with ailerons deflected, and with spoilers deflected ahead of the ailerons. Tests were also to be made to determine the downwash and the flow fluctuations behind the wing at stations corresponding to possible horizontal tail locations. It was agreed that data would be obtained at Mach numbers up to and including 0.90.

It was further agreed that the typical wing would have an NACA 65_1-210 section, an aspect ratio of 9.0, a taper ratio of 2.5 to 1.0, no sweepback, no twist, 3° of dihedral, and a tip similar to that of the P-51 airplane. It was to have a 20-percent-chord plain aileron that was to extend from the 60-percent-semispan station to the end of the straight portion of the trailing edge. Both straight-sided and beveled-edge ailerons were to be tested.

In order to make available to the Army and the design contractors the results of these investigations as soon as is practicable the results of previously outlined investigations are being presented in several reports. The results reported herein include the lift, moment, and drag data for the wing alone with straight-sided ailerons at 0° deflection and constitute part I of the series of reports.

SYMBOLS

Aerodynamic coefficient and other symbols used are defined as follows:

α	angle of attack
V	velocity in undisturbed stream
p_L	local static pressure at a point on airfoil section
p	static pressure in undisturbed stream
ρ	mass density in undisturbed stream
a	speed of sound in undisturbed stream
q	dynamic pressure $(1/2\ \rho V^2)$
P	pressure coefficient $\left(\frac{p_L - p}{q}\right)$
M	Mach number
c	chord ~~of model~~ in feet
b	span of model in feet
S	area of model in square feet
MAC	mean aerodynamic chord (4.45 inches)
A_T	area of tunnel cross section in square feet
L	lift on model
x	distance along chord from leading edge of section
y	distance along semispan from wing center line
z	vertical distance from center of wake-survey rake

Subscripts:

U	upper surface of airfoil section
L	lower surface of airfoil section

c_n section-normal-force coefficient

$$c_n = \frac{1}{c}\int_0^c (P_L - P_U)\, dx$$

c_m section-pitching-moment coefficient

$$c_m = \frac{1}{c^2}\int_0^c (P_U - P_L)\left(x - \frac{c}{4}\right) dx$$

C_N wing-normal-force coefficient

$$C_N = \frac{1}{S}\int_{-b/2}^{b/2} c\, c_n\, dy$$

$C_{M_{c/4}}$ wing-pitching-moment coefficient

$$C_M = \frac{1}{S(MAC)}\int_{-b/2}^{b/2} c^2 c_m\, dy$$

C_B wing-bending-moment coefficient

$$C_B = \frac{1}{S}\int_{-b/2}^{b/2} c^2 c_n y\, dy$$

C_{B60} bending-moment coefficient for outboard 40 percent of wing

$$C_{B_{60}} = \frac{2}{S}\int_{0.3b}^{0.5b} c^2 c_n\, dy$$

$2\,y_L/b$ lateral position of the center of wing lift

$$2y_L/b = C_B/C_N$$

C_{B60}/C_N center of lift coefficient for outboard 40 percent of wing

a_N slope of the normal-force curve $\left(dC_N/d\alpha\right)$

ΔH change in stream total-head pressure in wake

~~c_{d_p} point-drag coefficient~~

C_{D_o} wing-profile-drag coefficient

$$C_{D_o} = \frac{1}{b}\int_{-b/2}^{b/2}\int_{-10}^{10} cd_p \, dz \, dy$$

C_{D_i} wing-induced-drag coefficient

$$C_{D_i} = 0.036\, C_L^{\,2}$$

C_D total-wing-drag coefficient

$$C_D = C_{D_o} + C_{D_i}$$

APPARATUS

The Langley 8-foot high-speed wind tunnel, in which the tests were conducted, is of the single-return, closed-throat type. The Mach number at the throat is continuously controllable. The air-stream turbulence in the tunnel is small but slightly higher than in free air.

The model tested is shown in figure 1(b). The section, plan forms, aileron dimensions, and twist are those agreed upon. The model has been built with no dihedral however, in order to eliminate construction difficulties ~~which would have delayed the testing schedule.~~ The effective span of the model is 37.8 inches, the root chord is 6 inches, and the tip chord is 2.4 inches. Other dimensions, including those defining the tip shape, are given in figure 2 and table II. The ordinates of the NACA 65_1-210 airfoil used for the inboard sections are presented in table I. The ordinates of the sections of the outboard 40 percent of the wing ahead of the 80-percent-chord station are identical with those presented. From the 80-percent-chord station to the trailing edge, these sections have the ordinates of the straight-sided aileron. The model was machined from medium hard brass.

The ailerons were machined from steel and are attached to the wing by small hinges.

Twenty static pressure orifices were placed at each of eight chordwise stations along the span. The locations of these orifices chordwise at each station are presented in table III. The spanwise locations of the stations in percent of the semispan are 11, 20, 30, 43, 56, 64, 80, and 95. The four inboard stations were placed on the left half of the wing, the four outboard on the right half.

The model was supported in the tunnel by means of a vertical steel strut as shown in figure 1(a). The strut was specially designed to produce a uniform field of flow in the region of the model even at the extreme test Mach numbers scheduled. The profile of the strut is a modified ellipse, the ordinates for which are presented in table IV. The dimensions of the strut are given in figure 3. The strut is built up of four pieces; solid leading edge and trailing-edge plates and two cover plates over a hollow center portion. Static pressure orifices were placed at 30 points on this strut and 36 points on the tunnel wall. The model is placed at the center of the strut and extends from both sides. A rectangular center block with the dimension given in figure 2 was machined on the airfoil. This center block was fastened into a cut-out in a circular disk, the surfaces of which are flush with the surface of the strut as shown in figure 1(b). Two steel ears and a brass bearing are also fastened to this disk as shown in figure 3. The bearing is fitted into a bracket which is

fastened to the two cover plates. All lift and drag loads are taken by this bracket. Push-pull rods are connected to the ears and to a rocker arm at the top of the strut. A lever arm is attached to the rocker arm. The angle of model was changed during the tests by moving the lever arm through the required angle. The steel pressure tubes in the model were connected to tubes which passed through the hollow portion of the strut and were connected to multitube manometer boards.

Wake surveys were made by means of a rake placed behind the model as shown in figure 1(e) and 2. The rake has 42 total-pressure tubes and 7 static pressure heads. The vertical spacing of the total-pressure tubes varies from 0.1 inches at the center of the rake to 2 inches at the tips of the rake. The rake is supported in the tunnel by means of a horizontal strut.

TESTS

In order to insure the accuracy of the test results, a series of special calibration tests of the tunnel air stream were made with the support strut installed, both with and without the wake-survey-rake support strut installed. Static pressures were determined at 30 points on the strut and 36 points on the tunnel wall at Mach numbers up to 0.95 without and with the model in place. The tests with the model were made for angles of 0°, 4°, and 9°. A series of tests were also made to determine the static pressures and the angles of flow at the model position. A combination of a calibrated static head and a yaw head mounted on the wake-survey-rake support strut was used for these tests.

No force measurements were made during the tests of the model. All lift and moment data were obtained from pressure measurements, and all drag data were obtained from wake surveys. The pressure and wake measurements were made during separate test runs. Pressure measurements were made at the following Mach numbers and angles: for Mach numbers of 0.40, 0.60, 0.76, 0.80, 0.825, and 0.85 at angles of attack of -2°, 0°, 2°, 4°, 7°, and 10°; for Mach numbers of 0.90, 0.925, 0.95 at angles of attack of 0°, 2°, 4°, and 7°. The pressures at the 160 orifices in the wing were recorded simultaneously by photographing the manometer boards. Wake-survey measurements were made at

six vertical stations 1.4 root-chord lengths behind the 25-percent chord line of the wing. These stations were 20, 40, 60, 80, 95, and 102 percent of the wing semispan from the wing-support strut. These measurements were made for Mach numbers of 0.40, 0.60, 0.726, 0.76, 0.80, 0.85, and 0.882 at angles of attack of 0°, 2°, 4°, and 7°.

In order to obtain wake-width measurements at a typical tail location, wake surveys were made for a vertical station 2.82 root-chord lengths behind the 25-percent chord line of the wing and 5 inches from the strut.

RESULTS

Pressure Measurements

In order to illustrate the changes in the chordwise pressure distributions caused by compressibility effects, representative pressure distribution for the 30-percent semispan station are presented in figure 4 and similar data for the 95-percent-semispan station are shown in figure 5. The chordwise pressure diagrams for all the semispan stations have been integrated to determine section-normal-force coefficients and moment coefficients. These coefficients have been used to determine the spanwise variations in section loadings and moments. The spanwise variations in section loadings are presented in figure 6. The spanwise-load distributions have been integrated to determine the total normal forces and the moments of these forces about the root chord. The variations of the normal force with Mach number and angle of attack are presented in figures 7 and 8.

The slopes of the normal-force curves selected at lift coefficient values corresponding to a wing loading of 60 pounds per square foot at 35,000 feet have been determined and are presented in figure 9. The lateral positions of the centers of the lift on the wing in terms of the semispan are presented in figure 10. These values were obtained by dividing the values of the bending-moment coefficient by the corresponding values of normal-force coefficient. The lateral center of lift coefficients for

the outboard 40 percent of the wing semispan are presented in figure 11 to show the variations in the bending moments at the section at the root of the aileron where critical stresses may also occur. These coefficients were obtained by dividing the bending-moment coefficients for the 60-percent-semispan station by the normal-force coefficients for the entire wing. The lateral centers of lift on the wing in terms of the semispan have been determined for the various Mach numbers for the angles of attack that are needed to produce 180 pounds per square foot wing loading at 35,000 feet altitude, which corresponds approximately to a 3g dive recovery. The results are presented in figure 12.

The spanwise variations in section moments are presented in figure 13. The wing-pitching-moment coefficients based on the MAC have also been determined. The results are presented in figure 14 and 15.

Wake-Survey Measurements

The total-pressure measurements made during the wake surveys have been converted to $\Delta H/q$ form, and point-drag values have been determined by use of charts prepared at the Langley 8-foot high-speed wind tunnel. These values have been plotted against vertical distance for the various Mach numbers, angles of attack and rake stations in the wake, and integrated to obtain section-drag coefficients for these wake stations. These coefficients have been plotted against semispan and integration of the areas under these curves obtained have been used in the determination of the wing-profile-drag coefficient, based on the average wing chord of 4.2 inches. These results are presented in figures 16 and 17.

The profile-drag coefficients at normal-force coefficients corresponding to wing loadings of 60 and 80 pounds per square foot at 35,000 feet altitude for the various Mach numbers have been determined. The induced-drag coefficients for the same lift coefficients have been computed. The variations of the totals of the two drag coefficients with Mach number are presented in figure 18 for the two wing loadings.

The vertical variations of $\Delta H/q$ at a typical horizontal tail location, a station 2.82 root-chord lengths behind the 25-percent chord line and 5 inches from the strut are

presented in figure 19. Part of the wake-survey results obtained 1.40 root-chord lengths behind the 40-percent-semispan station are presented in figure 20 to show the rate of the vertical spread of the wing wake with distance. All wake dimensions are given in terms of the lengths of the chords behind which the measurements were made.

Effects of Reynolds Number

The Reynolds numbers obtained during the tests varied from 900,000 at a Mach number of 0.40 to 1,400,000 at a Mach number of 0.90. These values are considerably lower than those for a wing in flight. The effect of this variation at low Mach numbers may be estimated by comparing the data presented with that obtained during the tests of a similar wing in the Langley 19-foot pressure tunnel. All data previously obtained at supercritical Mach numbers indicate that at these Mach numbers the effects of variations in the Reynolds number are of minor importance in comparison with the predominating effects of compressibility.

Limitations of Test Mach Numbers

The tunnel chokes at the model at a calibration Mach number of 0.95 with the support strut and model in place. Numerous tests have indicated that the data obtained in a wind tunnel when it is choked at the model is not applicable to the prediction of wing characteristics for free air (reference 1). The data obtained at the choking Mach number of 0.95 have, therefore, not been presented. The data obtained at a Mach number of 0.925 are still being analyzed to determine the proper corrections with relation to the choking effects.

With the wake-survey-rake support strut in place the tunnel choked at this strut when the Mach number at the plane of the model was 0.882. As previously mentioned, a special calibration test was made with the wake-survey strut in place. The results of this test clearly show that no invalidating choking effects occur at the plane of the model when the tunnel chokes at the survey strut. Choking simply imposes a limitation on the maximum test Mach number instead of affecting the applicability of the results. The data on the model with the wake-survey strut in place can thus be assumed to be correct up to the choking Mach number of the wake-survey strut and data up to this point have been presented.

Calibration Test Results

A comparison of the static pressures measured on the surfaces of the strut, walls, and static pressure head during the calibration runs indicate that the Mach number and dynamic pressure gradients in the air stream at the model position are small. The variations in these values at the surface of the strut in the direction of the air stream are less than 0.2 percent through a distance of two feet at all Mach numbers up to 0.90. The variations in the vertical direction are less than 0.2 percent through a distance of four feet. The variations in the spanwise direction are less than 1.0 percent through a distance of 20 inches and 2.5 percent from the strut to the wall at Mach numbers up to 0.90. Weighted averages of all pressure measurements made near the model position have been used to determine the calibration curves for the test apparatus.

The angularity of the stream flow in a horizontal plane has been found to be less than 0.1°, this value being the limit of the accuracy of the calibrating instrument.

Corrections for Tunnel-Wall Interference

Calculations, ~~using the presently available methods,~~ have been made to estimate the magnitude of the effect of tunnel-wall interference on the Mach number, the dynamic pressure, and the lift, moment, and drag. Three types of interference have been considered:

(1) Solid blockage

(2) Wake blockage

(3) Lift vortex interference.

The basic formulae employed to determine the effects of solid blockage and lift vortex interference are taken from reference 2. Those for wake blockage have been taken from reference 3. Most of the corrections for effects of compressibility are from reference 4, while further corrections for these effects came from reference 5. The following expressions were used:

For the effects of ~~blockage:~~

$$\frac{\Delta V}{V} = \frac{0.0515}{A_T^{3/2}(1 - M)^2} \int_{-b/2}^{b/2} c^2 \, dy + \frac{(1 + 0.4M^2)}{4A_T\left(1 - M^2\right)^{3/2}} C_D S$$

$$\frac{\Delta M}{M} = \frac{\Delta V}{V}\left(1 + \frac{\gamma - 1}{2} M^2\right)$$

The dynamic pressures were corrected using the corrected velocity, $V + \Delta V$, and the usual isentropic flow relations.

For the effects of lift vortex interference:

$$\frac{\Delta C_L}{C_L} = \frac{\pi^2}{48} \frac{LC}{qA_T^{3/2}\left(1 - M^2\right)}$$

$$\frac{\Delta C_M}{C_M} = \frac{\pi^2}{192} \frac{LC}{qA_T^{3/2}\left(1 - M^2\right)}$$

$$\Delta\alpha = \frac{0.598\pi\left(LC + 4M_{c/4}\right)}{qA_T^{3/2}\sqrt{1 - M^2}} + \frac{1}{8}\frac{A}{S} C_L$$

$$C_{D_i} = \frac{1}{8}\frac{S}{A_T} C_L^2$$

The corrections to the coefficients listed above are in addition to the corrections for the change in q. The magnitude of the corrections obtained by the above methods have been found to be very small even at Mach numbers up to and including 0.90. At this Mach number, the correction required for the Mach number varies from 0.4 percent at an angle of attack of 0° to 1 percent at 10°. The corrections required in the values of the coefficients due to the changes in dynamic pressure are even smaller, the maximum correction needed being 0.3 percent. The corrections in the coefficients as calculated by the expressions for the lift vortex interference are of the same order of magnitude. The greater part of the corrections are due to wake blockage. The results obtained by the use of the above expression for the wake-

blockage corrections have been compared with wake-blockage corrections determined by use of measured static pressures at the tunnel wall and the results of the two methods have been found to agree within 20 percent at Mach numbers up to and including 0.90. It is, therefore, indicated that no large errors exist in the corrections applied. The corrections have been applied to all data for Mach numbers greater than 0.76. The corrections made in the values of the Mach numbers are indicated in figure 7 as the difference between the plotted Mach numbers and the test Mach numbers. In figures that present variations in coefficients for constant Mach numbers, average corrected Mach numbers are indicated.

Corrections for Model Inaccuracies

The dimensions of the chordwise sections of the model conform to those computed from the values given in table II within 0.003 inches. The maximum inaccuracies produced no measurable effect on the results. During the construction of the model a negative 0.3° twist developed in the right half of the wing. In addition, the wing was inadvertently tested with approximately a 0.3° negative aileron angle. The effects of these inaccuracies were clearly indicated by the results of the tests made at an angle of attack of -2° which is very close to the zero lift condition at low Mach numbers. The distributions for this angle at low Mach numbers were not zero across the span but showed a slightly negative normal force at the tip. All the normal-force results have been corrected for these inaccuracies by the use of cross plots of section-normal-force coefficient versus angle of attack.

The moment coefficients have also been corrected.

DISCUSSION

Normal-Force Characteristics

There are no important changes in the normal-force characteristics due to compressibility effects at Mach numbers below the point of force break, which varies from a Mach number of 0.73 at high angles of attack to 0.80 at 0° angle of attack. Beyond this Mach number there are large and in some cases erratic changes in the normal-force characteristics as indicated by figure 7. There is a rapid increase in the angle of zero lift. At a Mach number of 0.90 it amounts to 1° as compared to approximately -2° at subcritical Mach numbers. There is also a rapid decrease in the slope of the normal-force curve. These changes will produce severe effects on the trim and stability characteristics of an airplane with such a wing. The use of special control devices should be considered for flight Mach numbers above these critical values. Data showing the effect of such devices on this wing will be presented in the near future as another part of this investigation. For design conditions these changes occur at Mach numbers just above the maximum level-flight Mach number of 0.775 required by the Army. This wing is, therefore, of the maximum thickness possible with respect to obtaining satisfactory trim and stability characteristics at the maximum speed.

Figure 6(a) indicates that the spanwise-load distributions determined for low Mach numbers are nearly the same as that predicted by use of the charts presented in reference 7. These variations may be due to the effect of the wing tip shape or to effects of the aileron. Figure 6(b) indicates clearly that at 0.60 Mach number the outboard sections lose lift first when the angle is increased to 10°. At Mach numbers of 0.85 and 0.90 the distributions become extremely irregular at all angles of attack. At a Mach number of 0.90 the losses in lift at the tip sections are considerably less because of the effect of tip relief than at any of the inboard sections. Figure 10 indicates that for all angles of attack, producing positive lift, the lateral center of load moves outboard when the Mach number is increased beyond 0.775. Figure 12 indicates that, due to this general outboard shift in the load, the bending moment produced at the root of a wing with a loading of the magnitude that would occur during a rapid recovery from a dive (approximately 3g) is increased by 5 percent when the Mach number is increased from 0.775 to 0.90. This increase produces bending moments 2.5 percent greater than those predicted by the charts of reference 7. This fact should be considered when the design bending moments are calculated. This outboard movement in the center of lift may also contribute additional effects to the trim and stability characteristics of an airplane.

Figure 11 indicates that for a given change in Mach number the bending moments at the 60-percent-semispan station increases more rapidly than do those at the root section. If the maximum ~~point~~ stresses in the wing structure occur at this station, this fact must be considered.

The results IN FIGURE 8 indicate that lift coefficients corresponding to the probable maximum design loads can be obtained for this wing at the high test Mach numbers. It may be assumed, therefore, that in the estimation of maximum design conditions at these high Mach numbers that maximum lift will not limit the design conditions.

PITCHING Moments

There are extremely large, and in some cases erratic, changes in the pitching moments when the Mach number is increased beyond the point of force break as indicated in figure 14. There are large increases in the negative moments when the Mach number is increased to 0.83. At this Mach number the negative moment coefficients for the angles corresponding to design lift coefficients are more than -0.07. When the Mach number is increased beyond 0.83, the moments for the various angles diverge rapidly. At 0.90 Mach number the pitching moment for 7° is -0.117 while that for 2° is 0.012. Figure 15 indicates that the stability of the wing increases gradually up to a Mach number of 0.83. Beyond this point it increases rapidly.

Because of these changes in the moment coefficients, the moments about the neutral axis of the wing sections at high Mach numbers are less than those at low Mach numbers. It follows that the twists of the wing at these high numbers are less than the twists calculated by use of moment coefficients for low Mach numbers and the dynamic pressures for these high Mach numbers. The twist of this wing or one similar to it may be determined at any Mach number up to 0.90 by using the data presented in figure 13.

Drag

Figure 18 indicates that for a level-flight wing loading of 60 pounds per square foot for conditions at an altitude of 35,000 feet the drag rises abruptly when the Mach number is increased beyond a value of 0.79. This value is 0.035 Mach number above the high-speed level-flight Mach number for these conditions. It is 0.040 below the Mach number desired for design high speed, however. This comparison indicates that an airplane with a wing similar to that tested cannot fly at the desired Mach number unless it has a considerable margin of power above that needed for the cruising conditions. The results indicate that increases in the values of the drag coefficients occur at Mach numbers considerable higher than those that will be attained at the desired cruise conditions. It may be assumed, therefore, that the range of an airplane with a wing similar to that tested will not be seriously affected by the drag increases due to compressibility. It should be noted that an airplane with a 12-percent-thick section of the same type and camber will experience a similar drag rise at a Mach number of 0.765. This indicates that an airplane with such a wing cannot fly at the desired Mach number without a large excess of power, ~~above that required for cruise~~. An increase in the wing loading from 60 to 80 pounds per square foot does not change the Mach number at which the drag rise occurs by an

appreciable amount. A comparison of the data for the two wing loading on the basis of lift ~~over~~ drag ratios indicates that for any supercritical Mach number, the drag for a given lift is less for the higher wing loading of 80 pounds per square foot than for the lower loading of 60 pounds per square foot.

Wake Widths

Figure 19 indicates that for all angles of attack, the wake width at a vertical station near the probable tail location increases rapidly when the Mach number is increased beyond the critical. For an angle of attack of 2° at a Mach number of 0.882 the wake extends to a point 0.35 chord lengths above the wing chord line. The extension is not beyond the region of presently used tail locations. For the higher angles of attack used to recover from high-speed dives, however, the wakes extend to a point at least 0.7 chord lengths above the wing chord line. In order to reduce the probabilities of tail buffeting and losses in tail effectiveness, it is imperative that the tail be placed at least 0.7 chord lengths above the wing chord line.

A comparison of the results of figure 20 with those in 19 indicates that the wake behind the wing spreads rapidly at supercritical Mach numbers. At an angle of attack of 7° at a vertical position 1.4 chord lengths behind the 25-percent chord line, the wake width is equal to approximately 0.5 chord lengths for a Mach number of 0.85. For the same angle and Mach number but at a station 2.82 chord lengths behind 25-percent chord line, the wake width is equal to approximately 0.75 chord lengths. The divergence

of the edges of the wake is about 10° for this condition.

At a Mach number of 0.90 the divergence is about 12°.

At 0.76 it is only 3°.

CONCLUDING REMARKS

1. At Mach numbers above the point of force break, which varies from a Mach number of 0.73 at high angles of attack to a Mach number of 0.80 at 0° angle of attack, serious changes occur in the angles of zero lift and the slopes of the lift curves.

2. There are outboard shifts in the lateral centers of lift for all angles of attack when the Mach number is increased beyond 0.775. The outboard shifts produce approximately a 5-percent increase in the bending moment at the root section for high wing-loading conditions.

3. There are large increases in the negative pitching-moment coefficients when the Mach number is increased from that of force break to a value of 0.83. When the Mach number is increased beyond 0.83, moments for the various angles diverge rapidly with a resulting increase in stability.

4. There is a considerable rise in the values of the drag coefficients for the approximate lift coefficients needed to maintain level flight when the Mach number is increased beyond a value of 0.79.

5. The wakes at the probable fore-aft tail location extend to points at least 0.7 root chord lengths above the chord line for the angles of attack required to recover rapidly from a dive at Mach numbers of 0.85 and higher.

Langley Memorial Aeronautical Laboratory
National Advisory Committee for Aeronautics
Langley Field, Va., May 29, 1945

Richard T. Whitcomb
Aeronautical Engineer

Approved:

John Stack
Chief of Compressibility Research Division

REFERENCES

1. Byrne, Robert W.: Experimental Constriction Effects in High-Speed Wing Tunnels. NACA ACR No. L4L07a, 1944.

2. Glauert, H.: Wing-Tunnel Interference on Wings, Bodies, and Airscrews, British ARC, R and M No. 1566, 1933.

3. Thom, A: Blockage Corrections and Choking in R.A.E. High-Speed Tunnel. British R.A.E. Report No. Aero 1891, Nov. 1943.

4. Goldstein, S. and Young, A.D.: The Linear Perturbation Theory of Compressible Flow, with Applications to Wind-Tunnel Interference. British ARC, 1943.

5. Allen, H. Julian and Vincenti, Walter G.: Effect of Wall Interference in a Two-Dimensional Flow Wind Tunnel. NACA ARR, 1944.

6. ANC-1(1): Spanwise Air-Load Distribution. Army-Navy-Commerce Committee on Aircraft Requirements, Apr. 1938.

TABLE I

ORDINATES FOR NACA 65,-210 AIRFOIL
Stations and ordinates in percent of wing chord

Upper Surface		Lower Surface	
Station	Ordinate	Station	Ordinate
0	0	0	0
.435	.819	.565	-.719
.678	.999	.822	-.859
1.169	1.273	1.331	-1.059
2.408	1.757	2.592	-1.385
4.898	2.491	5.102	-1.859
7.394	3.069	7.606	-2.221
9.894	3.555	10.106	-2.521
14.899	4.338	15.101	-2.992
19.909	4.938	20.091	-3.346
24.921	5.397	25.079	-3.607
29.936	5.732	30.064	-3.788
34.951	5.954	35.049	-3.894
39.968	6.067	40.032	-3.925
44.984	6.058	45.016	-3.868
50.000	5.915	50.000	-3.709
55.014	5.625	54.986	-3.435
60.027	5.217	59.973	-3.075
65.036	4.712	64.964	-2.652
70.043	4.128	69.957	-2.184
75.045	3.479	74.955	-1.689
80.044	2.783	79.956	-1.191
85.038	2.057	84.962	- .711
90.028	1.327	89.972	- .293
95.014	.622	94.986	.010
100.000	0	100.000	0

L. E. radius:.016.099. Slope of radius through end of chord: 0.084

TABLE II

DIMENSIONS OF WING TIP SHAPE IN INCHES

Plan form contours		
Distance from tip X	Y_F	Y_T
0	-0.360	0.360
.026	.041	.963
.053	.176	1.168
.079	.268	1.307
.105	.337	1.413
.158	.436	1.565
.236	.529	1.710
.341	.595	1.817
.473	.623	1.868

Section contours		
Distance from tip X	Y_U	Y_L
0.026	0.024	0.076
.053	.041	.093
.079	.052	.105
.105	.061	.113
.158	.074	.126
.236	.086	.138
.341	.094	.147
.473	.098	.151

TABLE III

CHORDWISE LOCATIONS OF STATIC PRESSURE ORIFICES
Stations in percent of wing chord

Upper surface	Lower surface
2.0	3.0
6.0	10.0
15.0	25.0
27.5	41.0
40.0	52.5
50.0	62.5
59.0	72.5
67.5	84.5
77.5	94.5
88.0	
94.0	

The orifices on the aileron are not exactly at these locations.

TABLE IV

ORDINATES FOR CROSS SECTION OF SUPPORT STRUT

Station	Ordinate
Distance from 50-percent chord station to leading edge (in.)	Distance from chord line (in.)
0	0.37500
2.50	.37300
5.00	.36750
7.50	.35800
10.00	.34400
12.50	.32525
15.00	.30125
17.50	.26925
18.75	.25025
20.00	.22700
21.25	.19975
21.875	.18675
22.50	.16550
23.125	.14450
23.75	.11875
24.375	.08475
24.687	.05975
24.75	.05350
24.875	.03775
24.950	.02490
25.00	0
Leading edge radius =	0.0055

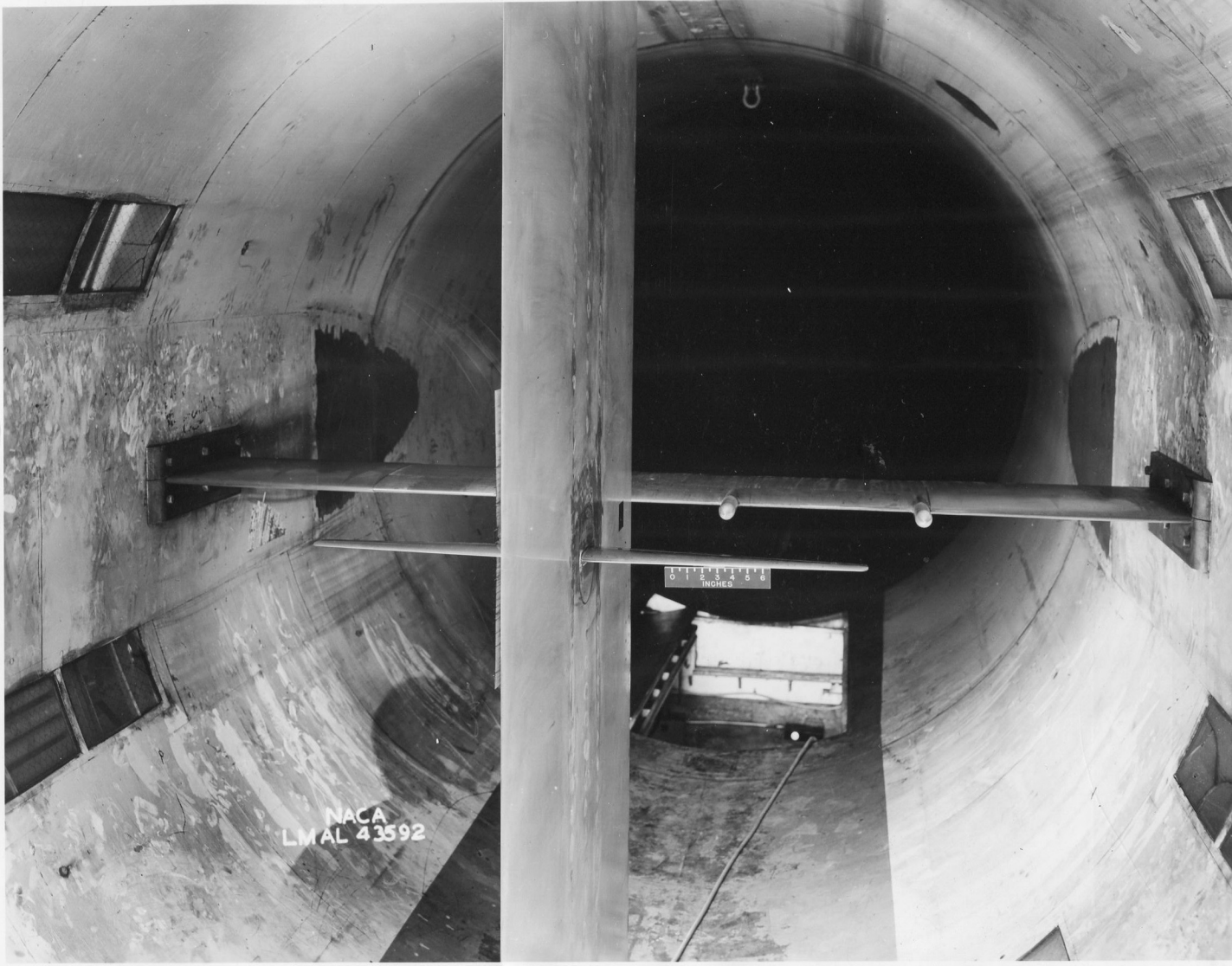

(a)

Figure 1.- Test apparatus.

NATIONAL ADVISORY COMMITTEE FOR AERONAUTICS
LANGLEY MEMORIAL AERONAUTICAL LABORATORY - LANGLEY FIELD, VA.

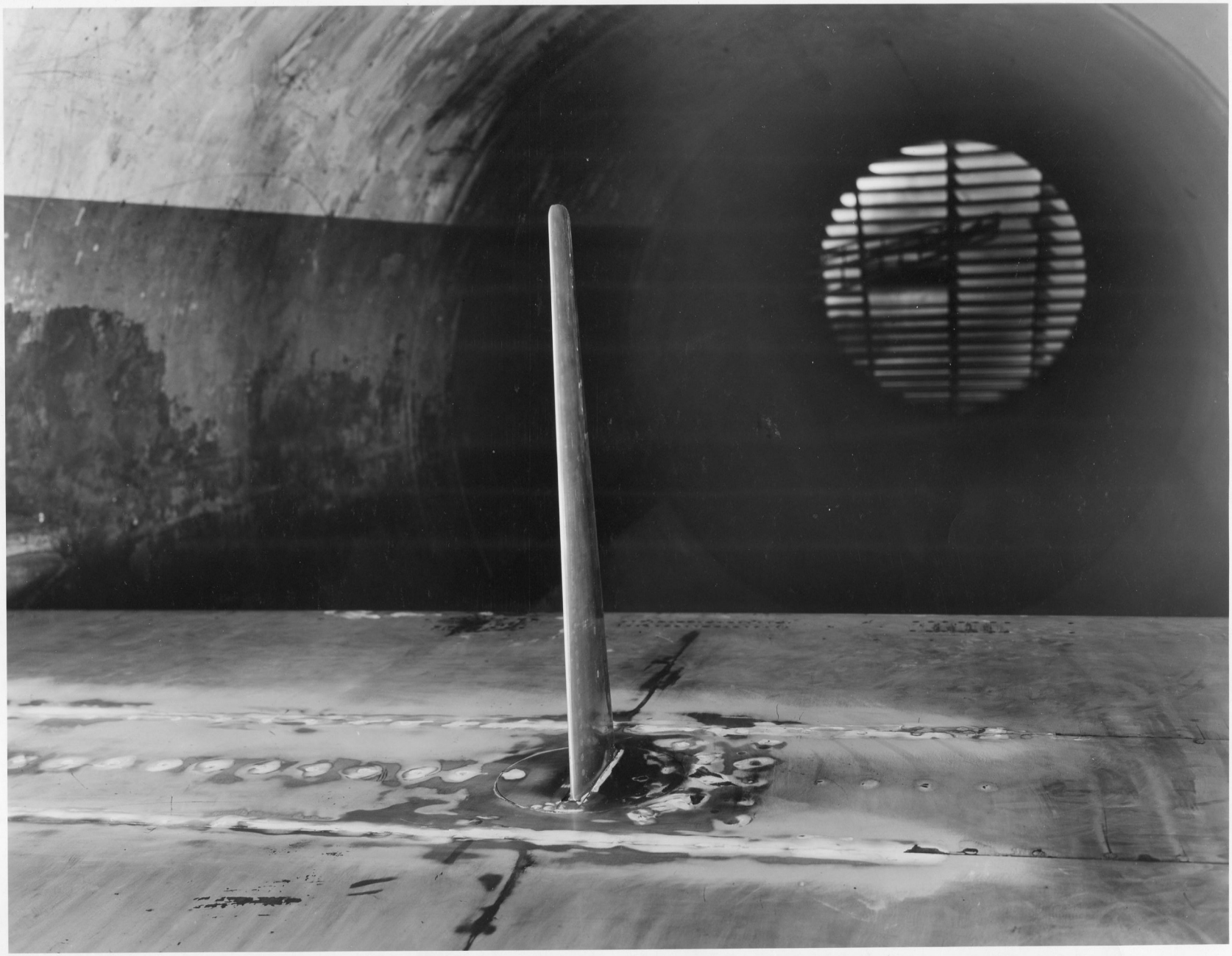

(b)

Figure 1.- Continued.

(c)

Figure 1.- Concluded.

NATIONAL ADVISORY COMMITTEE FOR AERONAUTICS
LANGLEY MEMORIAL AERONAUTICAL LABORATORY · LANGLEY FIELD, VA

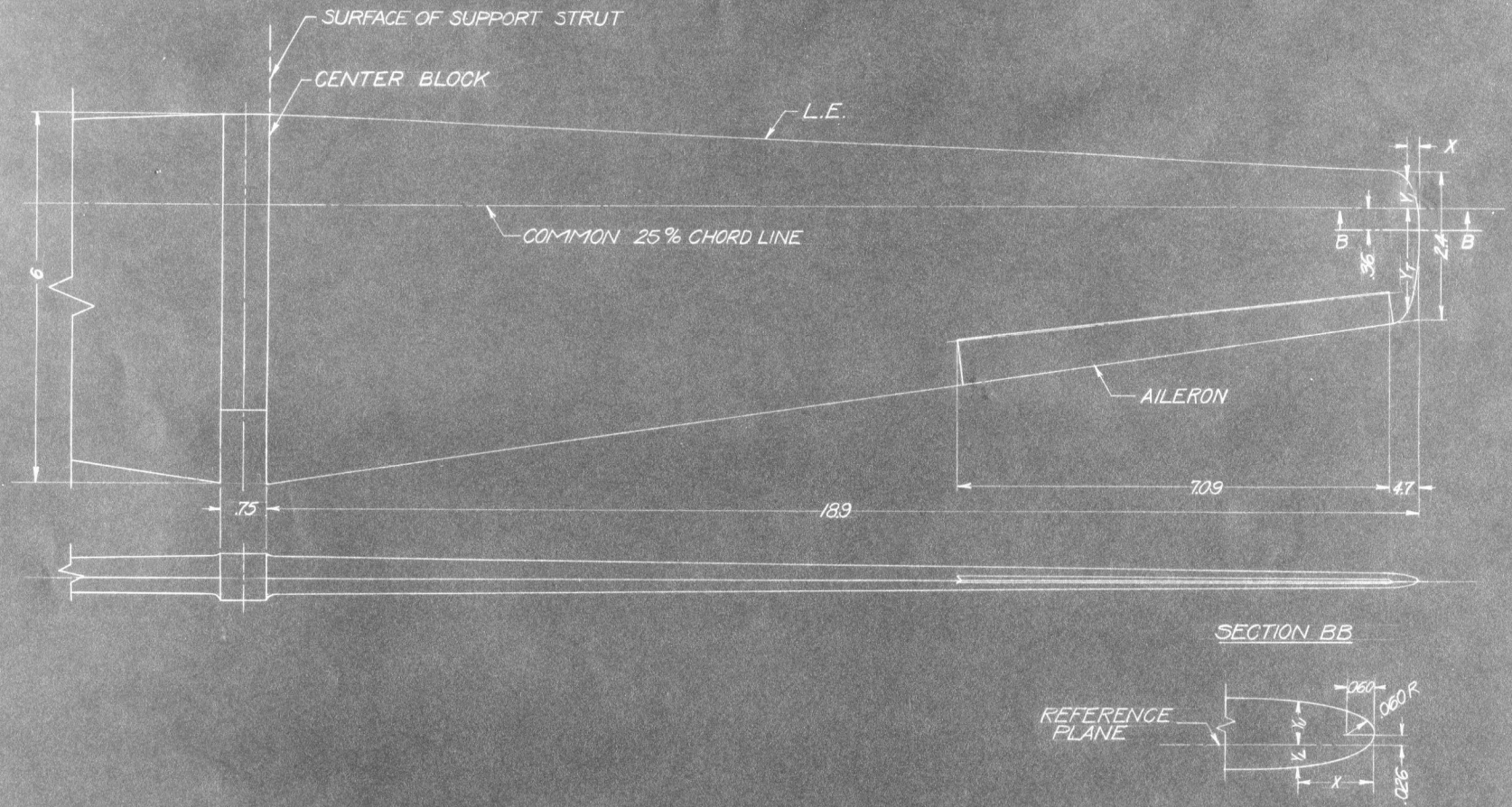

FIGURE 2.—WING DIMENSIONS.

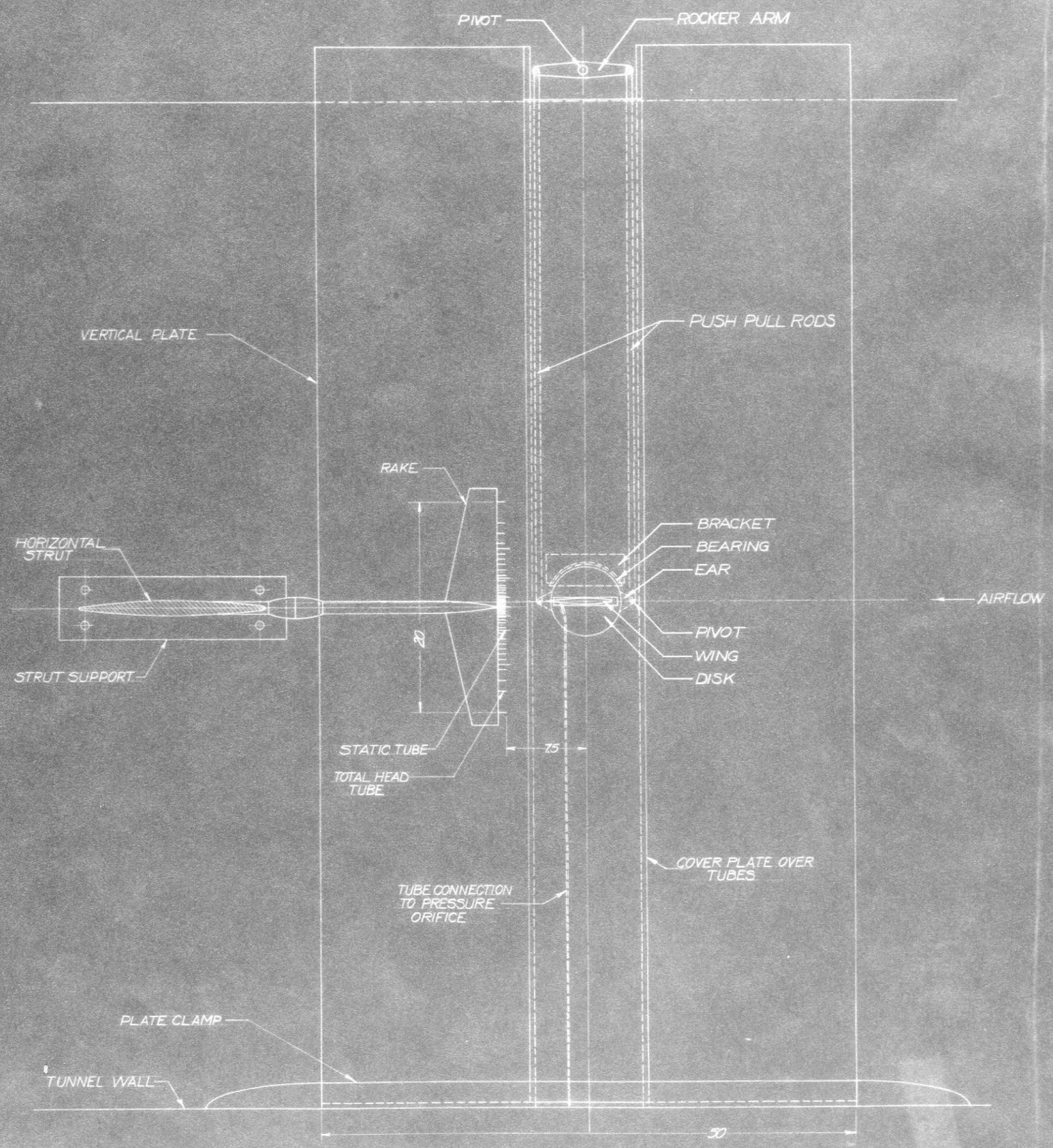

FIGURE 3.—COMPLETE TEST APPARATUS.

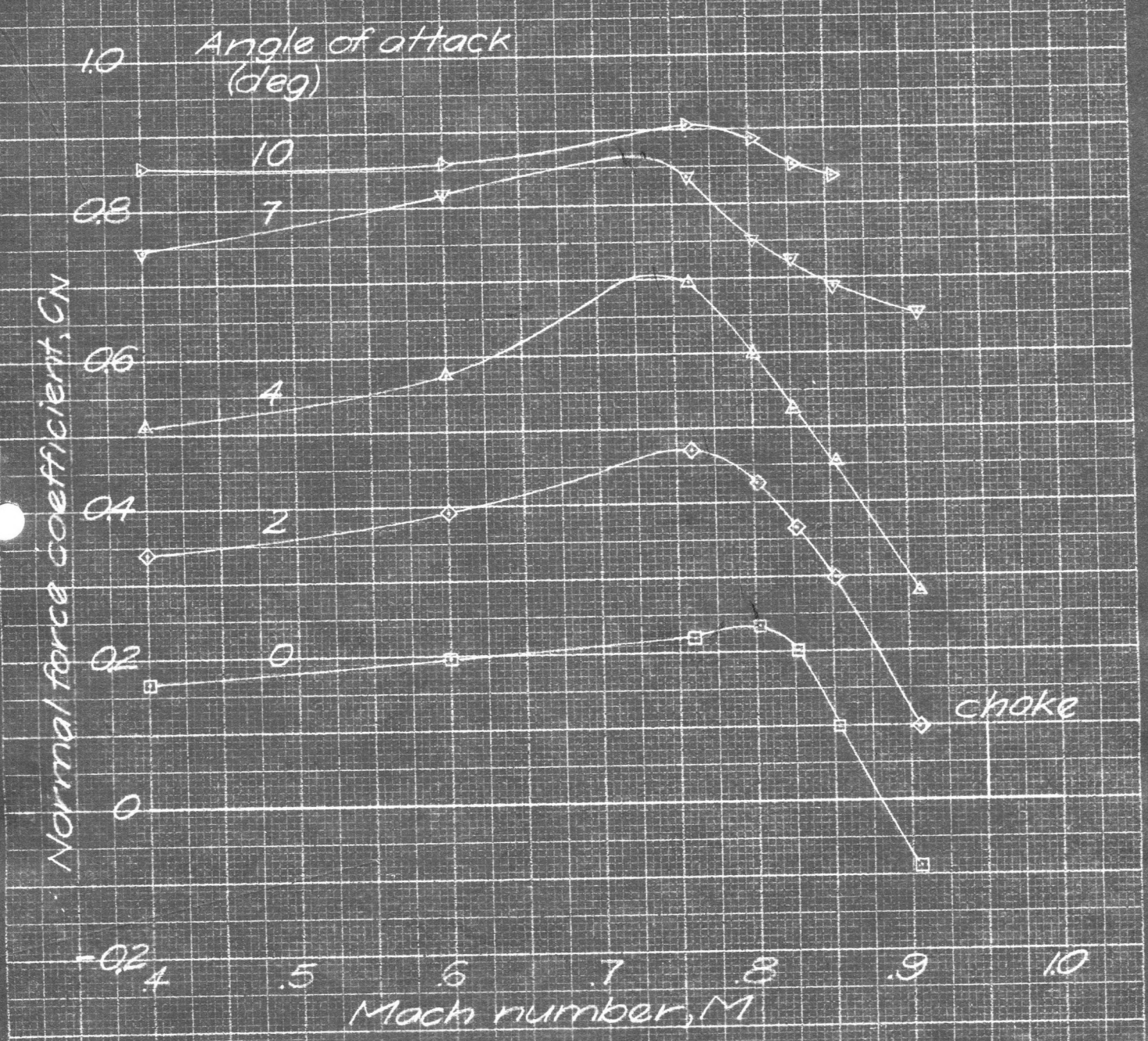

Figure 7 — Variation of wing normal force coefficient with Mach number.

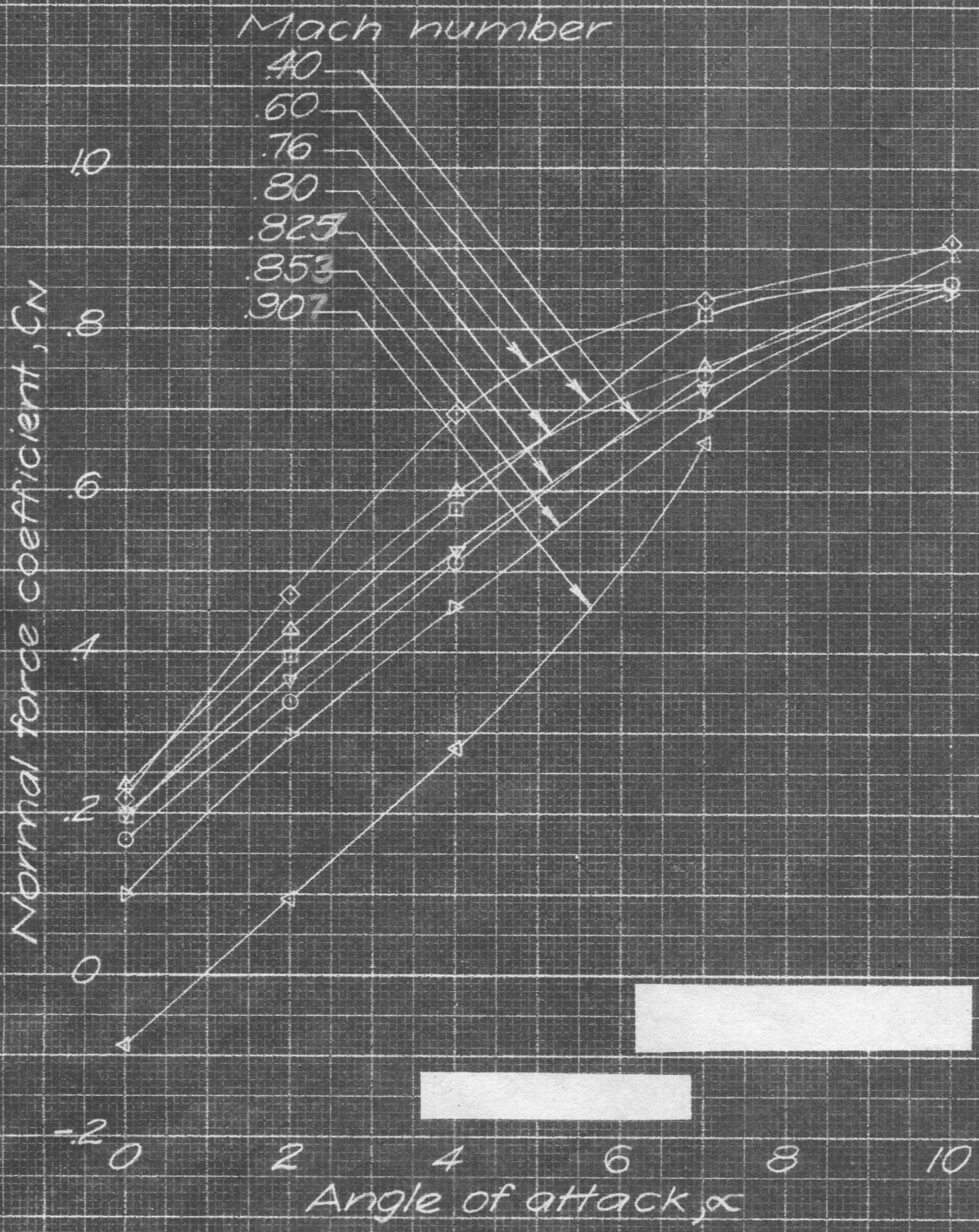

Figure 8 – Variation of normal force coefficient with angle of attack.

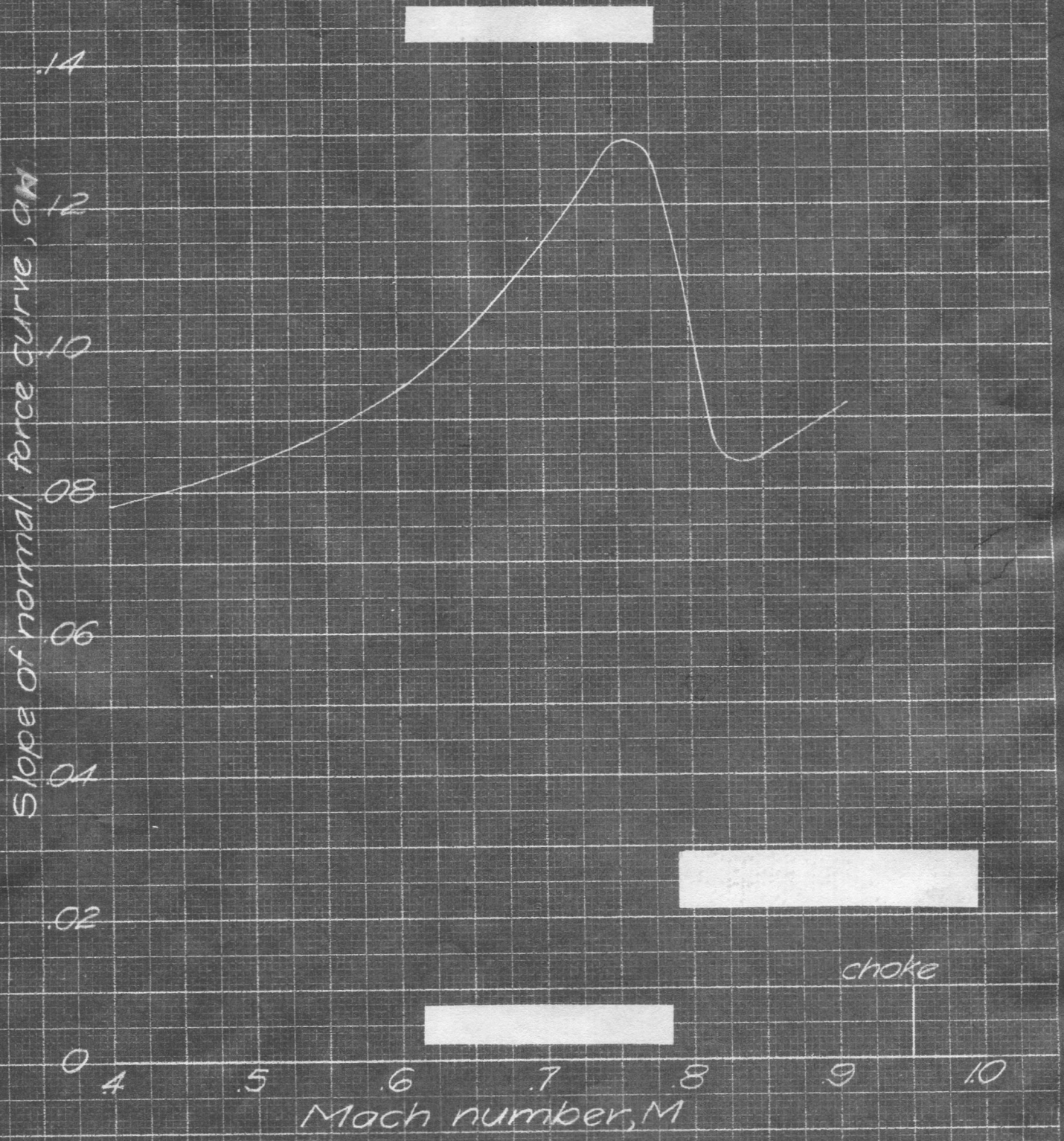

Figure 9 — Slope of normal force coefficient curve for 60 pounds per square foot loading at 35,000 feet altitude.

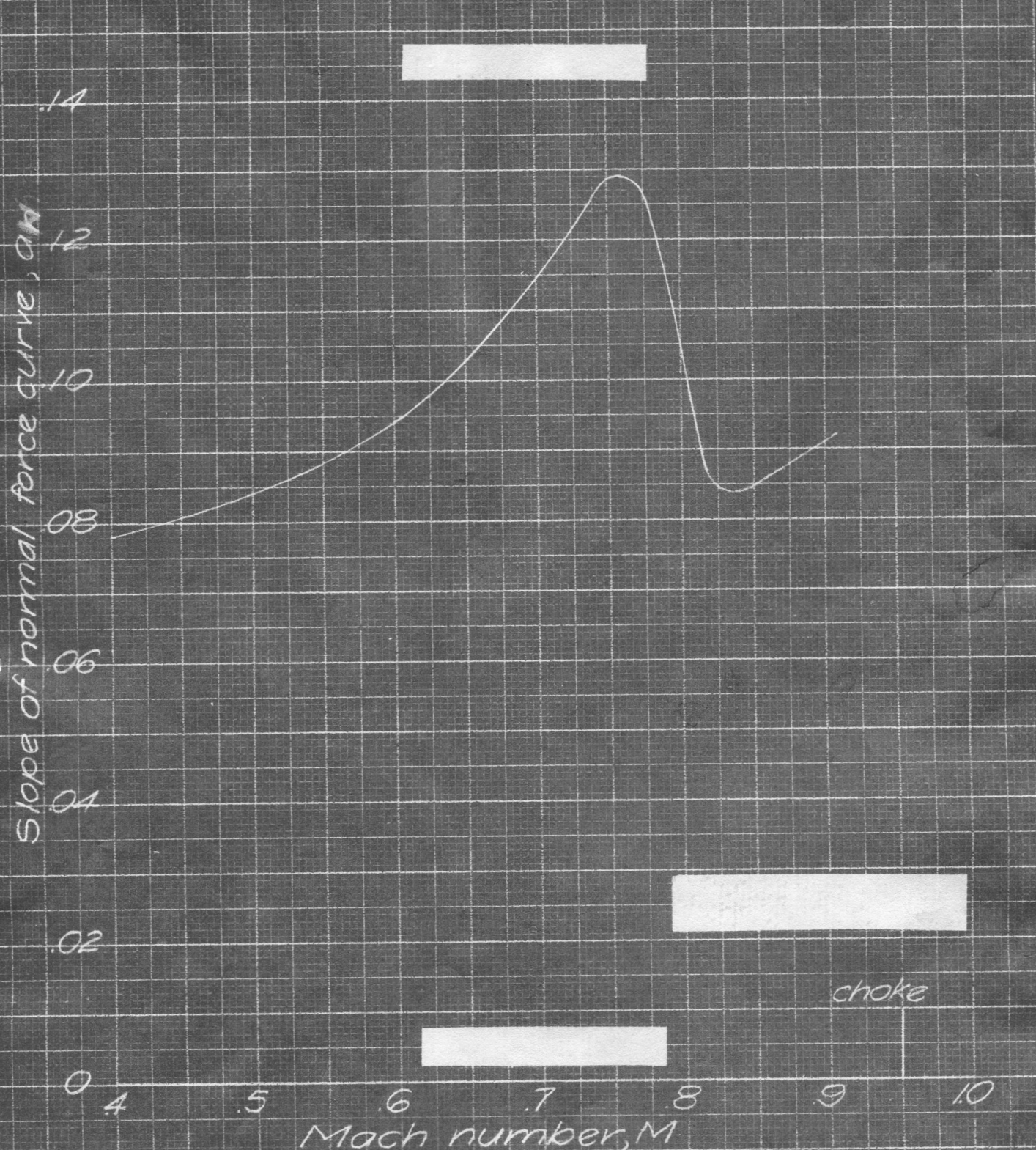

Figure 9 — Slope of normal force coefficient curve for 60 pounds per square foot loading at 35,000 feet altitude.

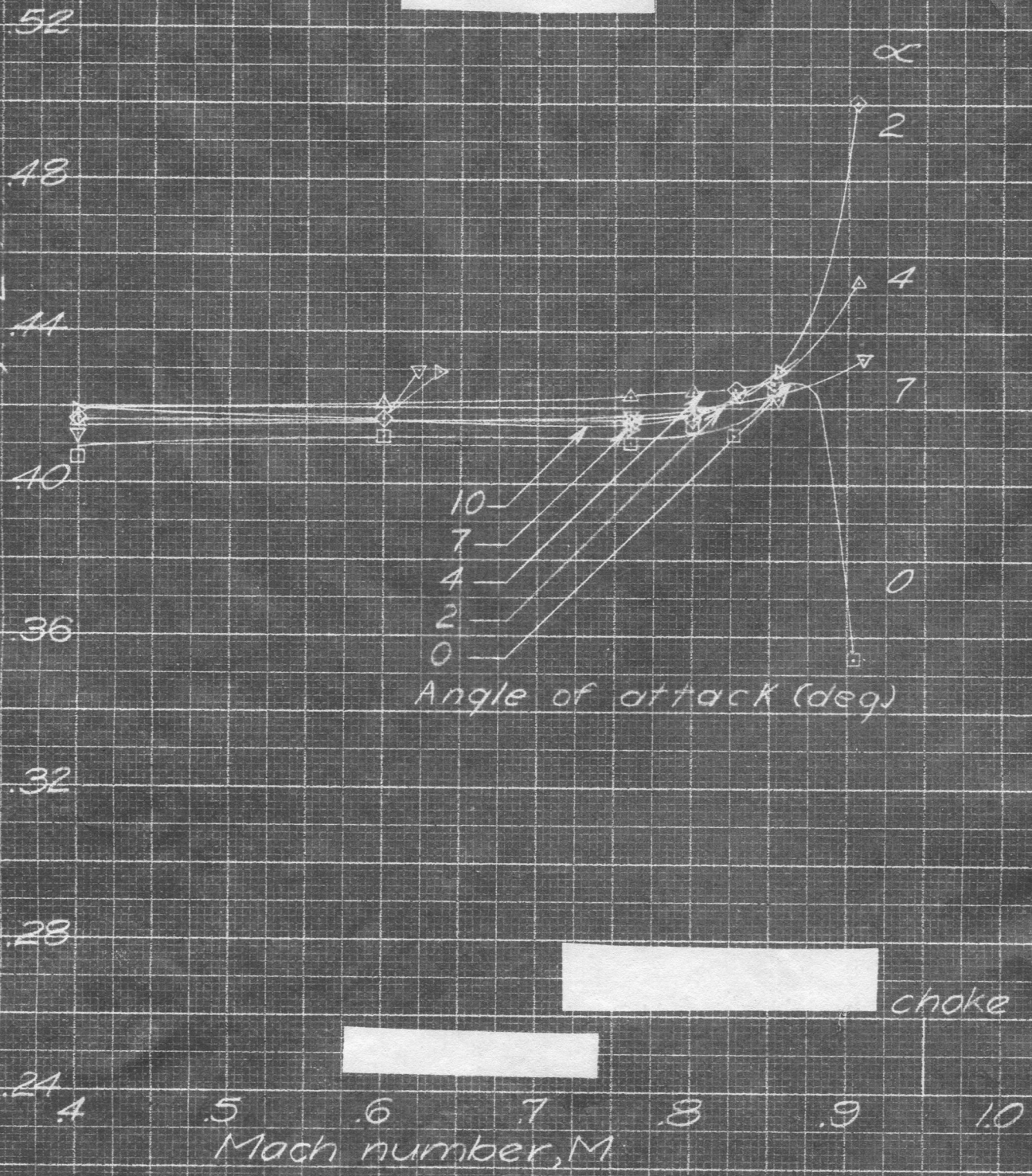

Figure 10 – Variation of wing center of lift coefficient with Mach number.

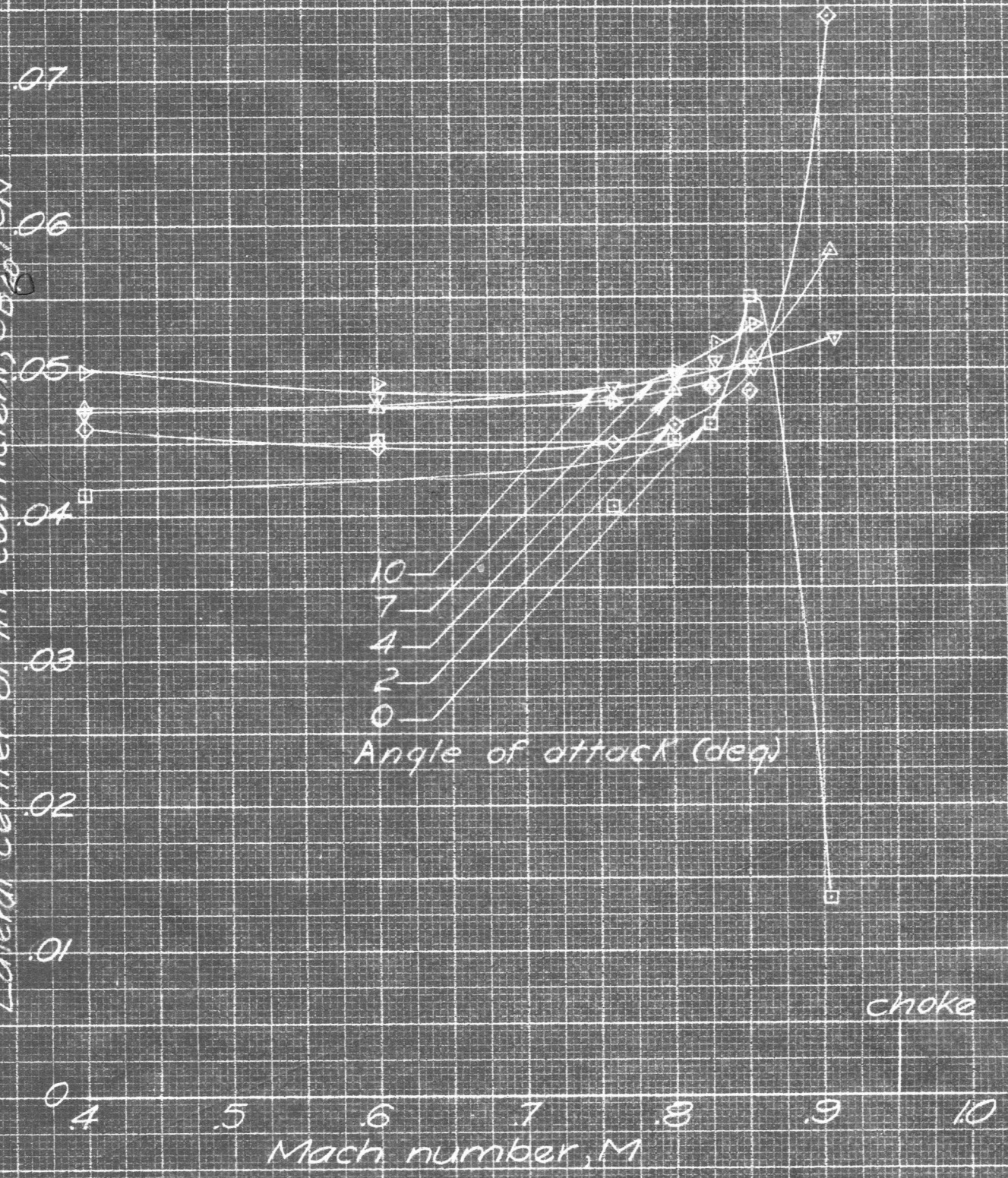

Figure 11 — Variation of tip center of lift coefficient with Mach number.

for outboard 40 percent of wing

Figure 12 — Variation of wing center of lift coefficient with Mach number for a wing loading of 180 pounds per square foot at 35,000 feet altitude

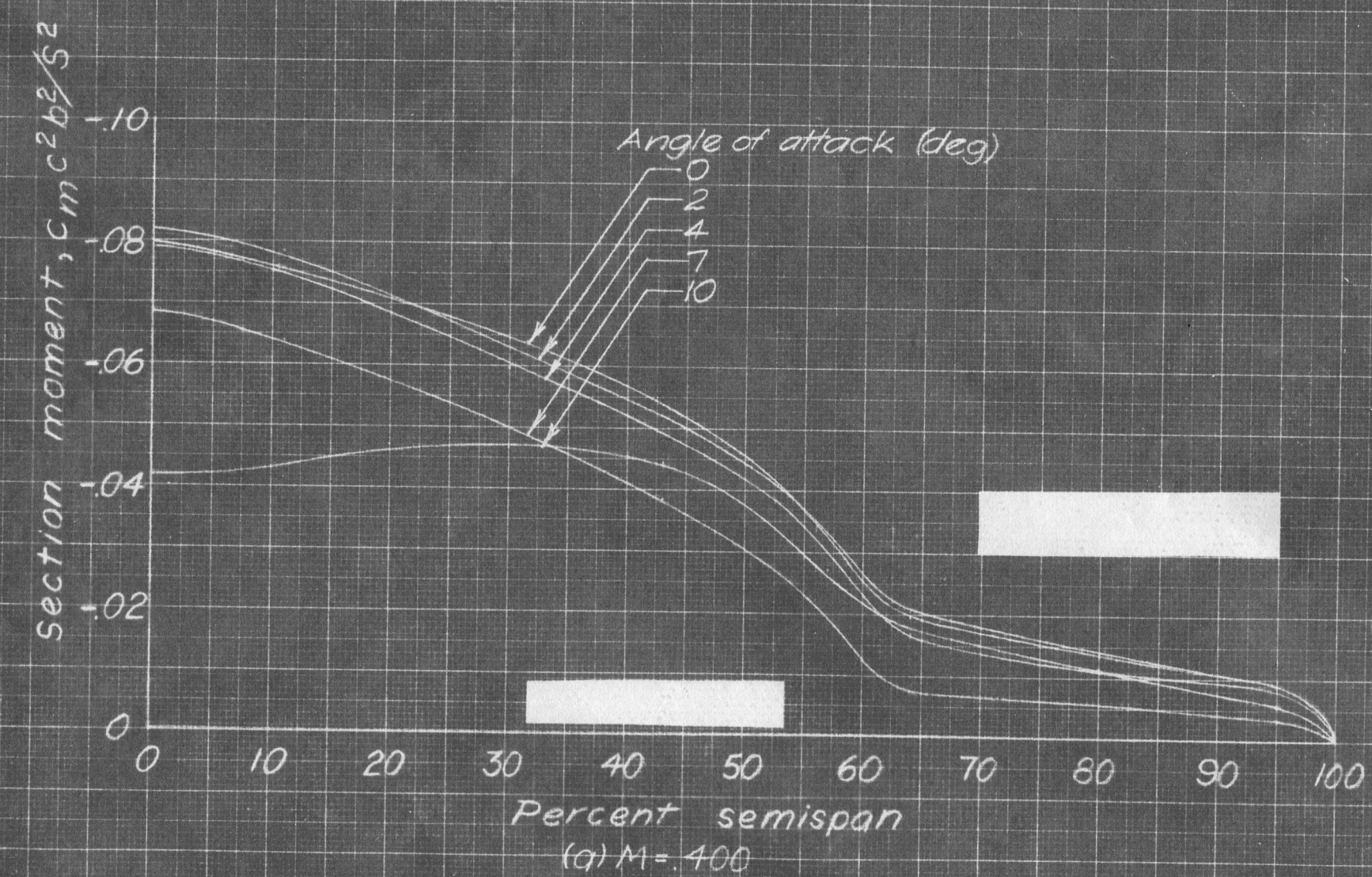

(a) M = .400

Figure 13- Spanwise variation in section moment.

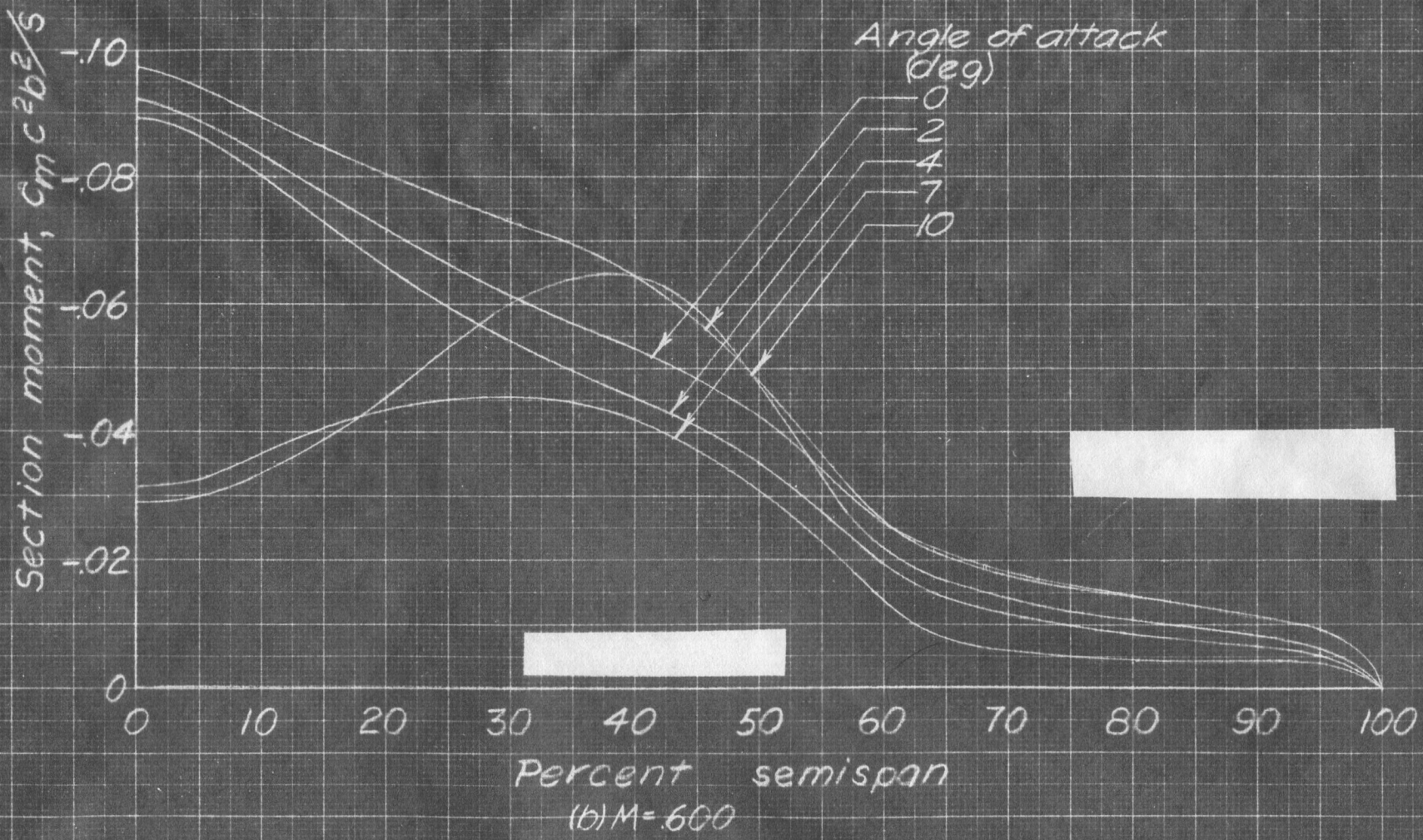

(b) M = .600

Figure 13 - Continued.

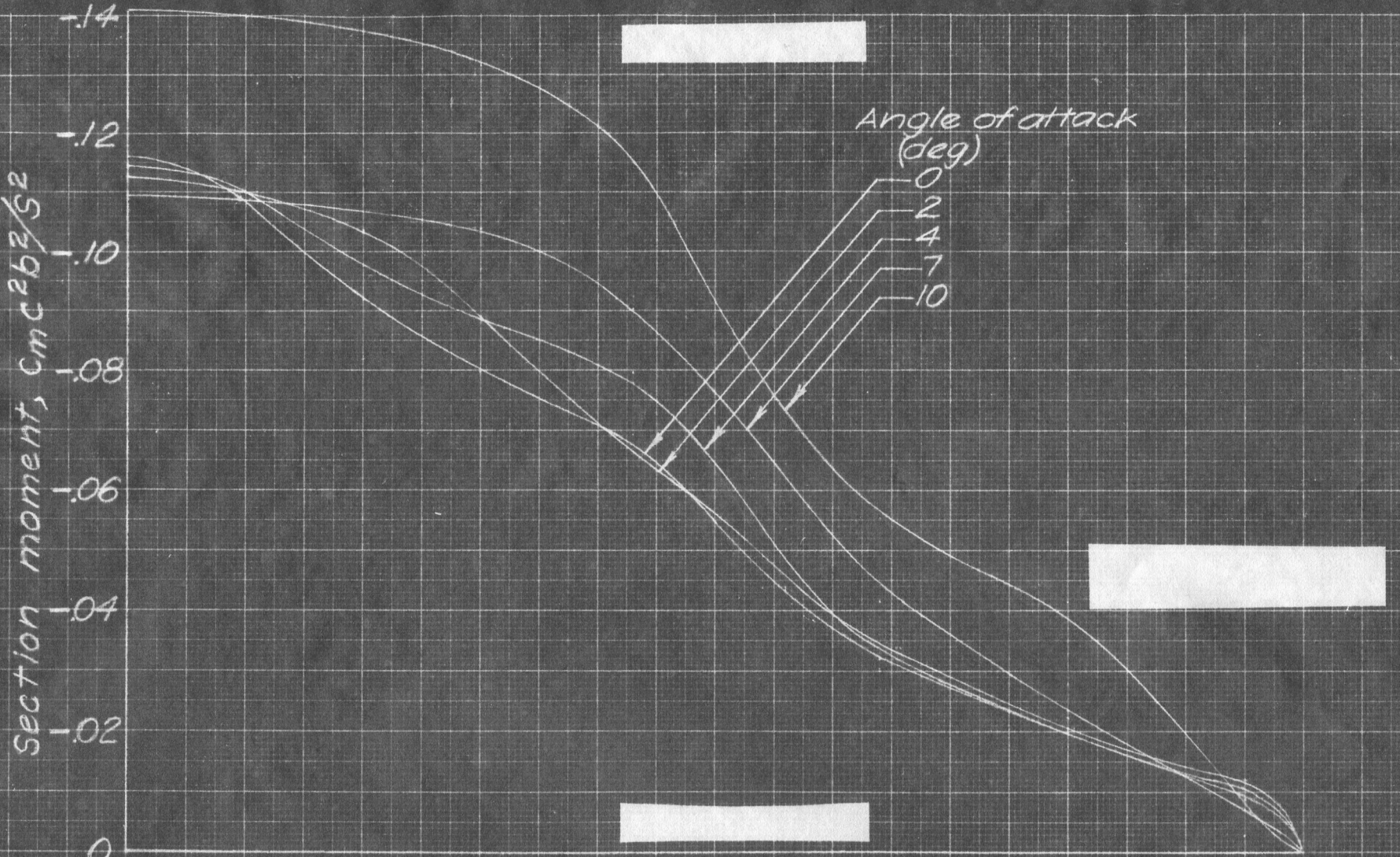

(c) M = .760

Figure 13-Continued

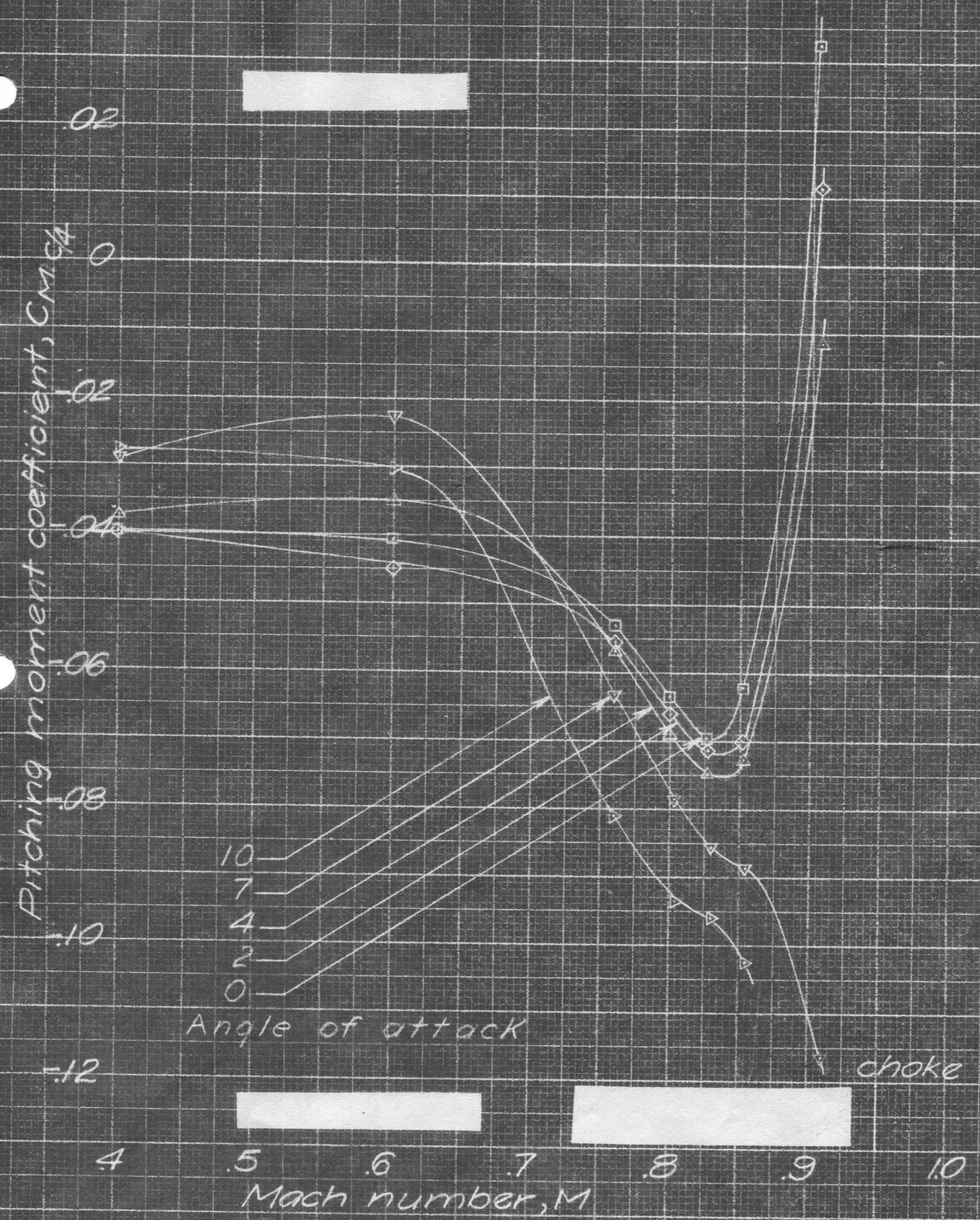

Figure 14 – Variation of wing pitching moment coefficient with Mach number.

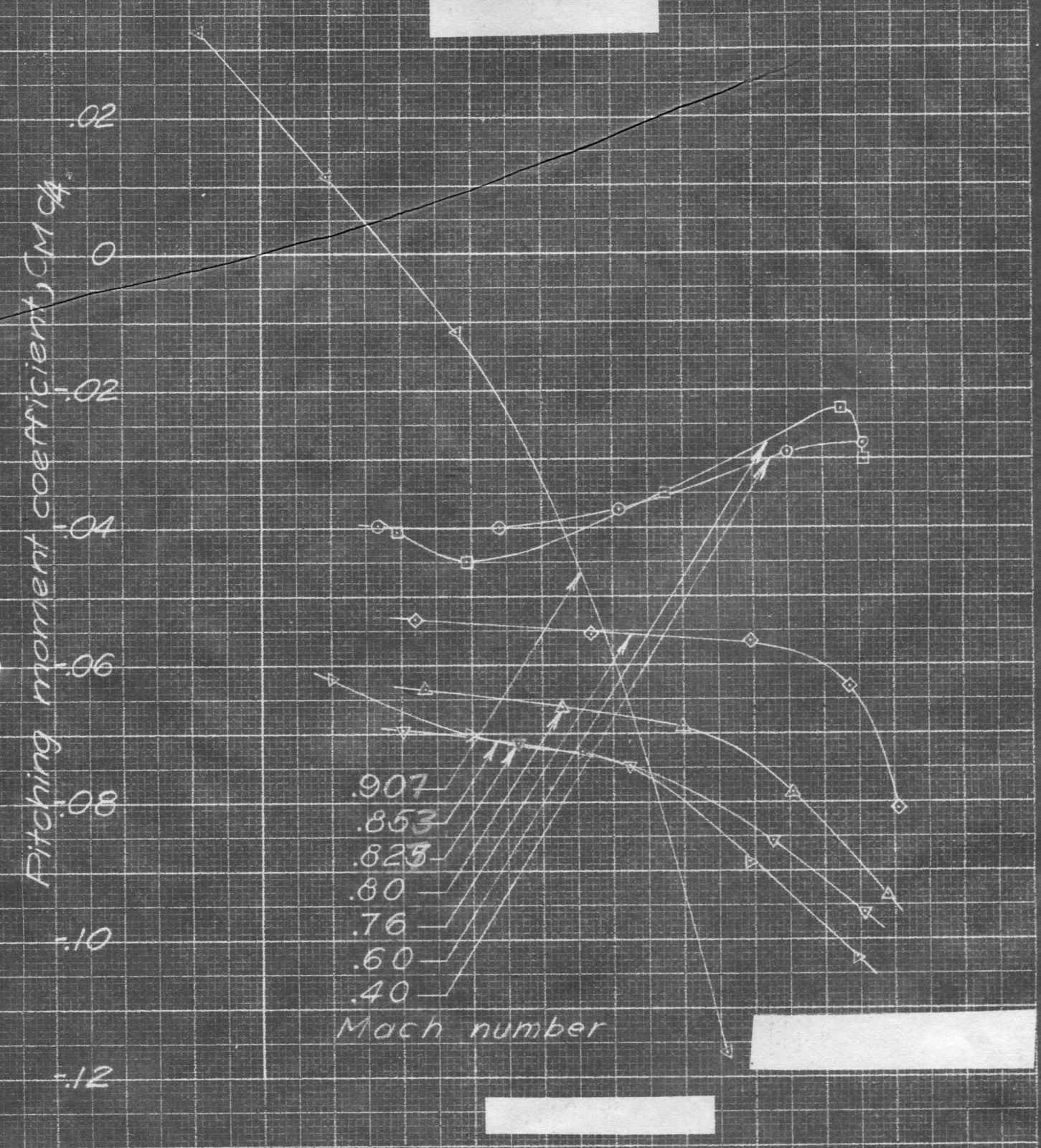

Figure 15 - Variation of wing pitching moment coefficient with normal force coefficient.

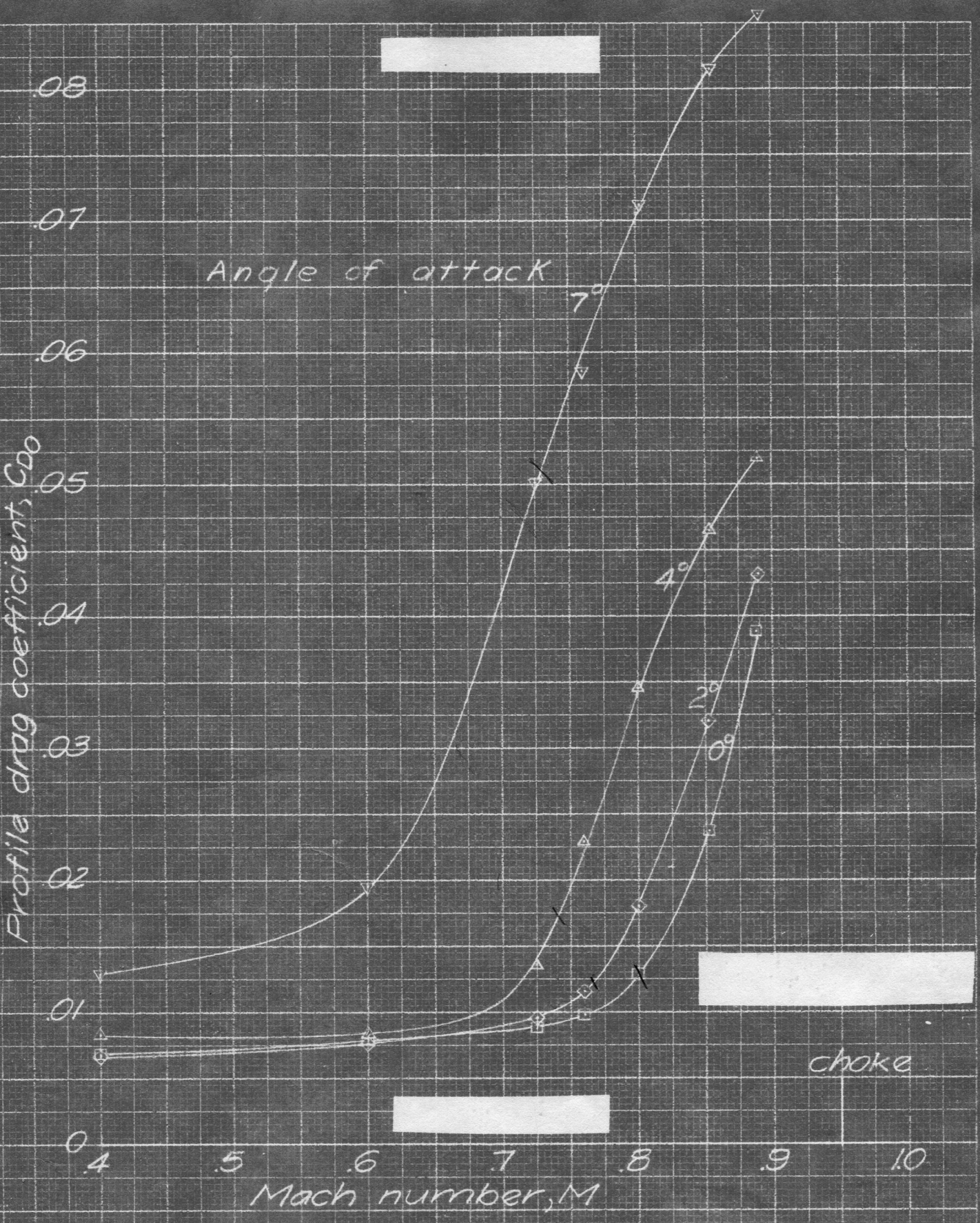

Figure 16 – Variation of wing profile drag coefficient with Mach number.

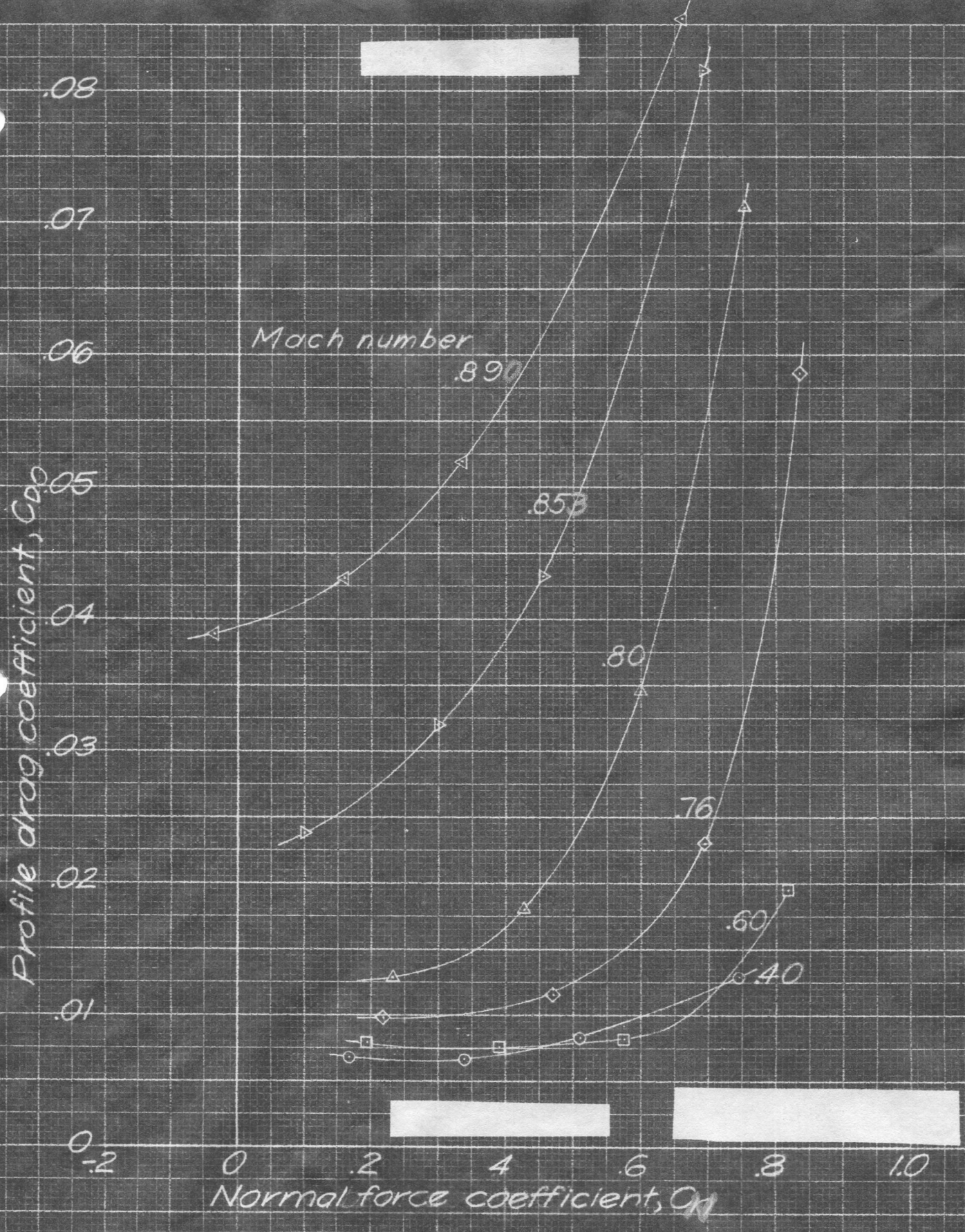

Figure 17 — Variation of wing profile drag coefficient with normal force coefficient.

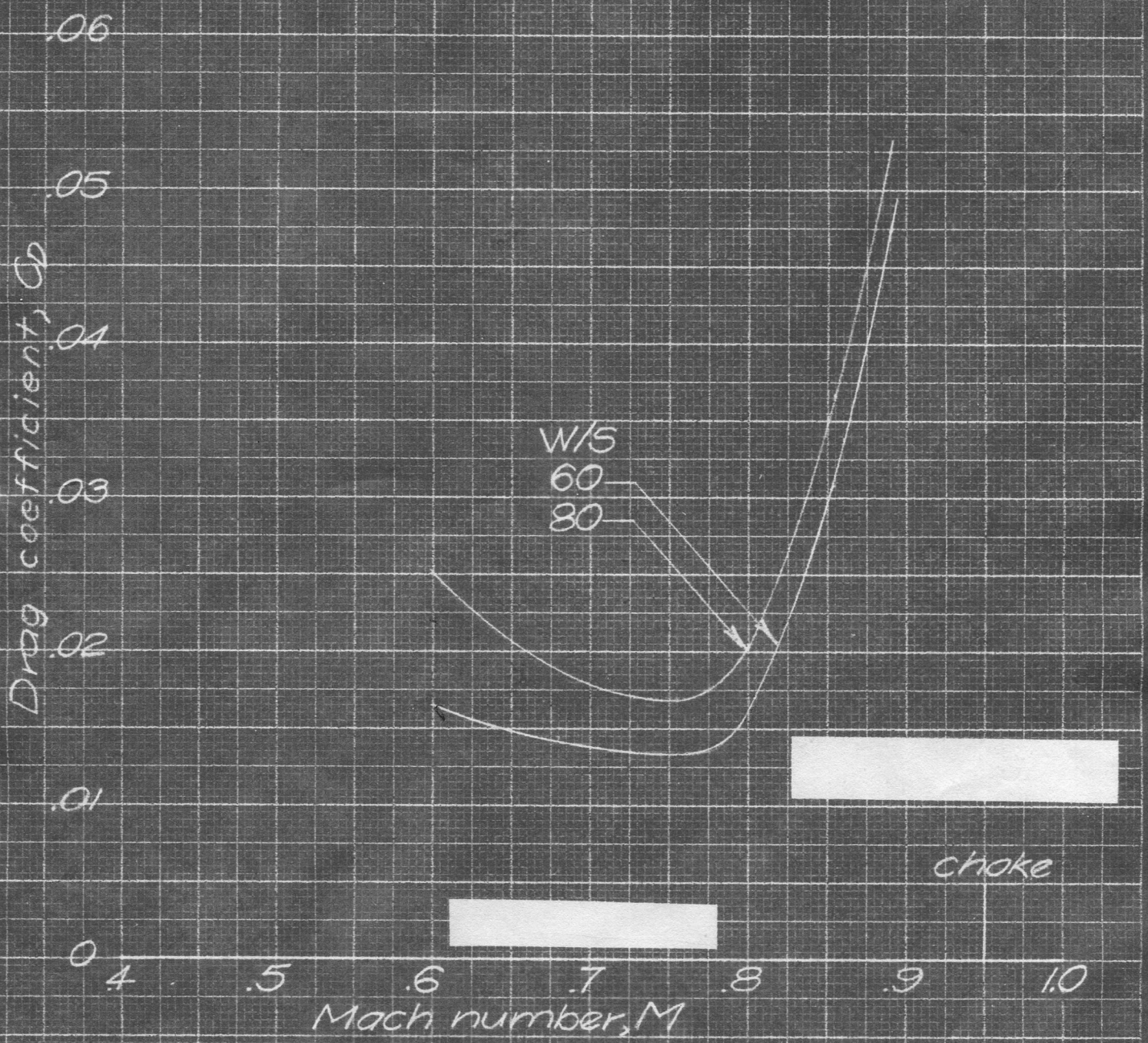

Figure 18 — Variation of drag coefficient with Mach number for wing loadings of 60 and 80 pounds per square foot at 35,000 feet altitude (calculated induced drag included).

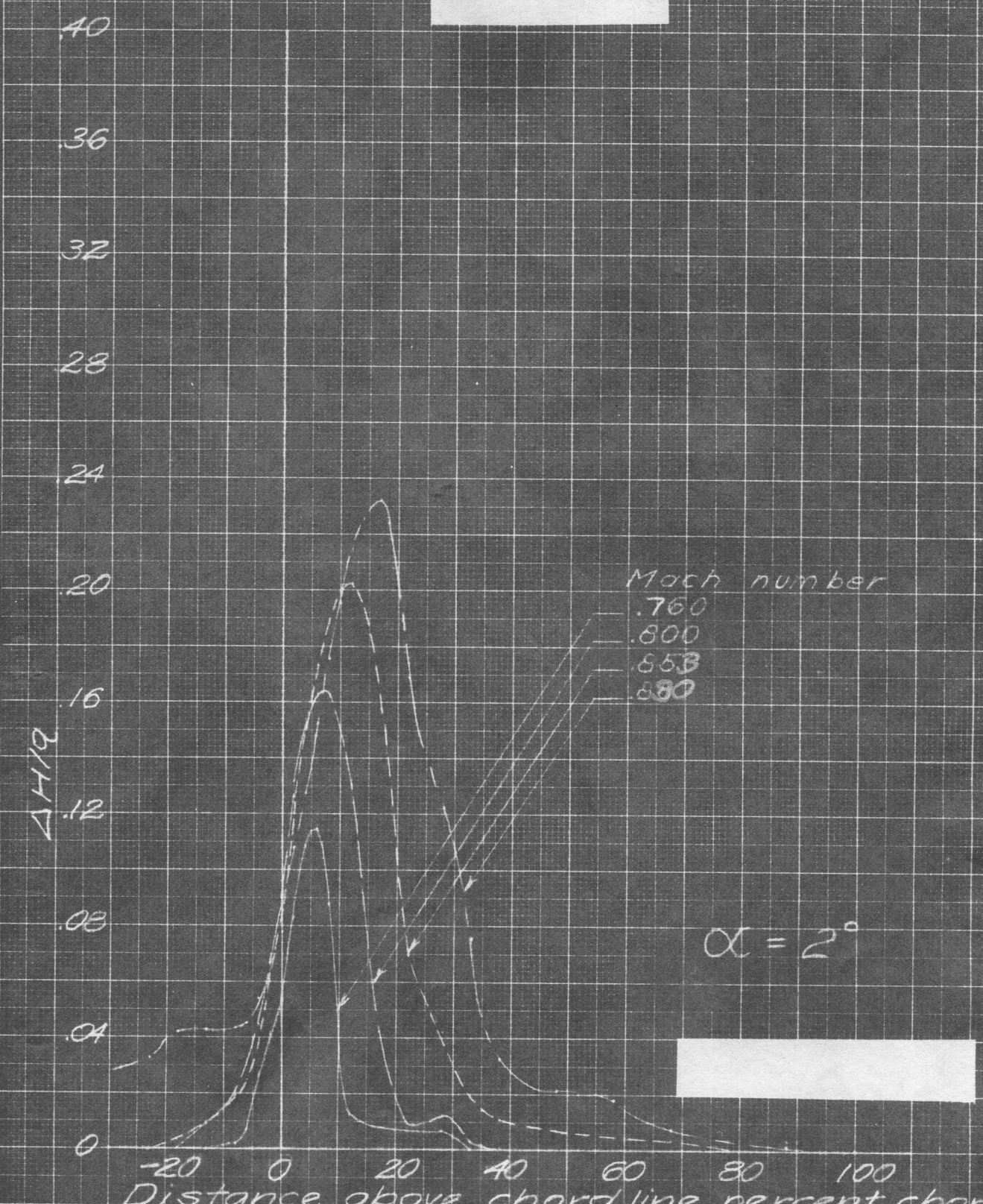

Figure 19 – Wake widths for several Mach numbers 2.82 root chord lengths behind the 25 percent chord line.

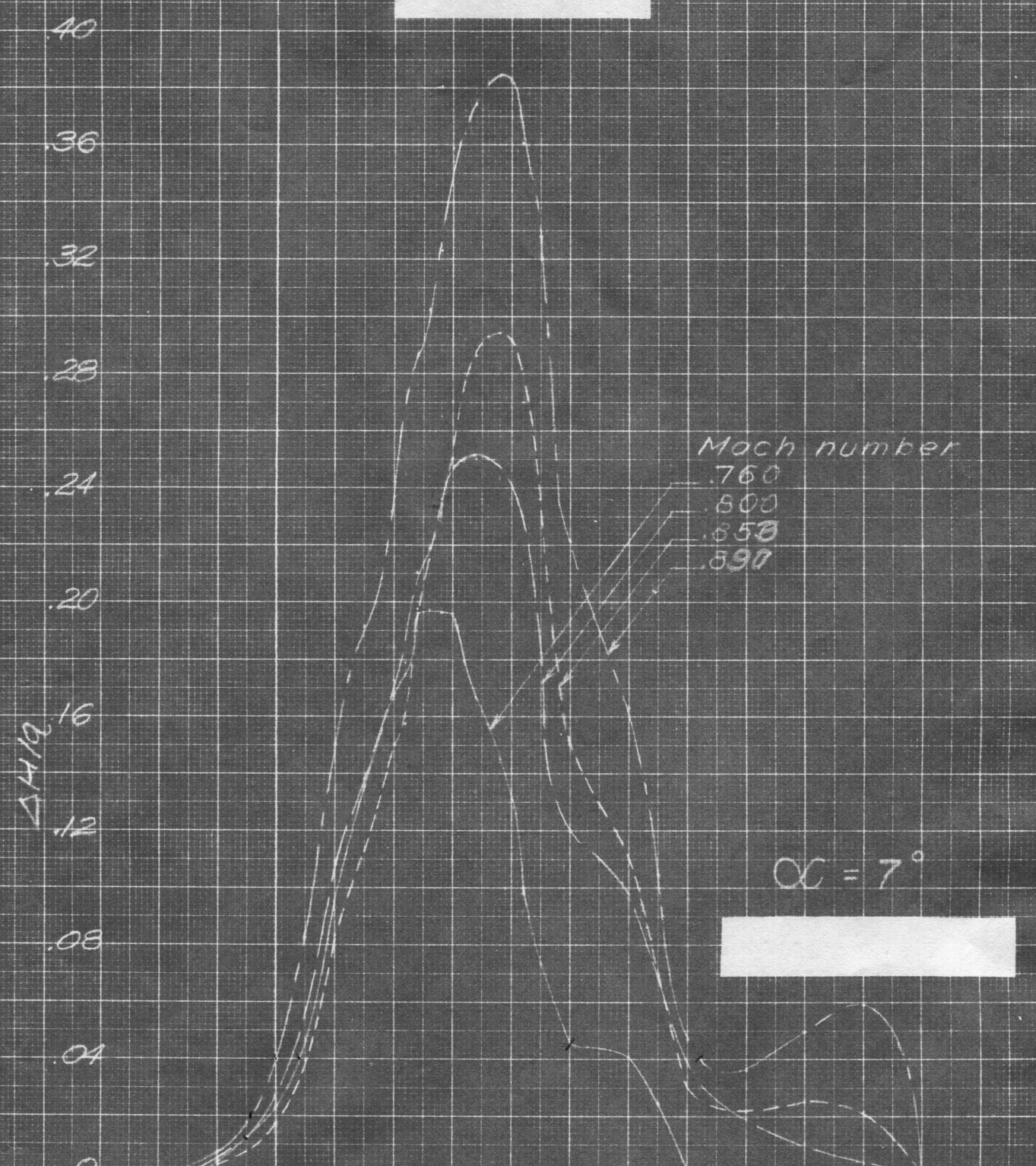

Figure 19 – Continued.

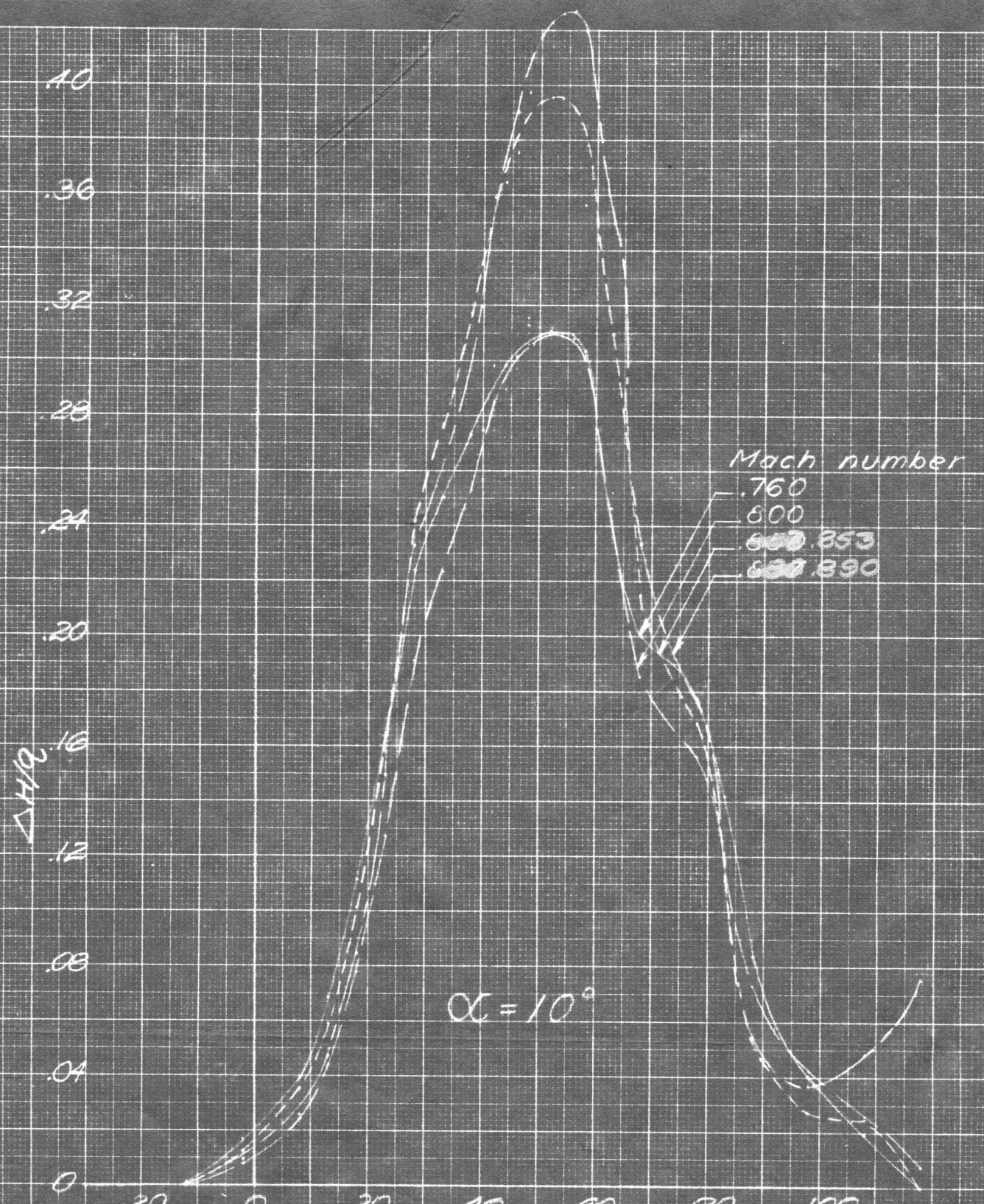

Figure 19 - Concluded.

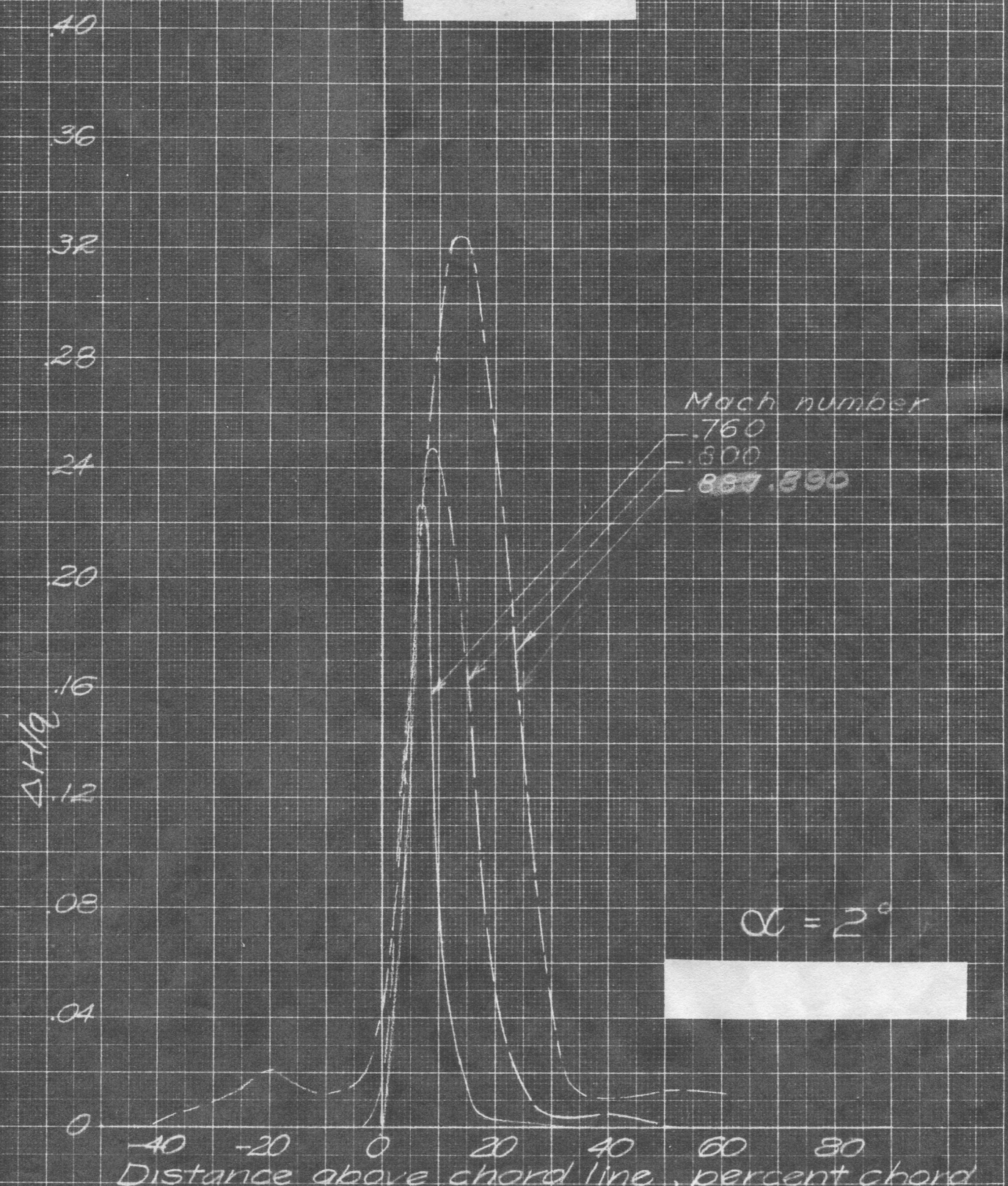

Figure 20 — Wake widths for several Mach numbers 1.40 root chord lengths behind the 25 percent chord line.

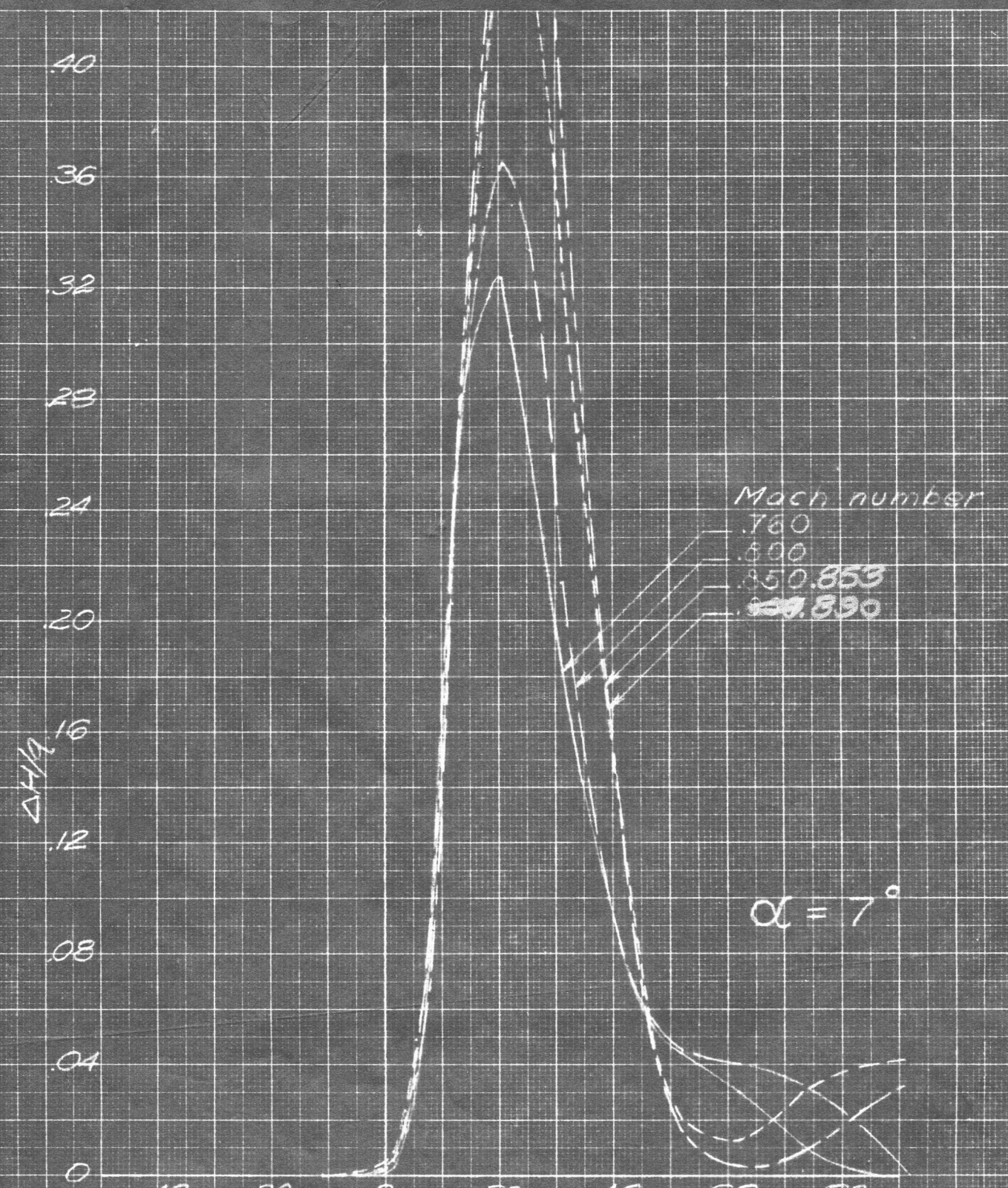

Figure 20 — Concluded.